NUREG/CR-6411
PNL-10866

A Geostatistical Methodology to Assess the Accuracy of Unsaturated Flow Models

Prepared by
J. L. Smoot, R. E. Williams

Pacific Northwest National Laboratory

Prepared for
U.S. Nuclear Regulatory Commission

AVAILABILITY NOTICE

Availability of Reference Materials Cited in NRC Publications

Most documents cited in NRC publications will be available from one of the following sources:

1. The NRC Public Document Room, 2120 L Street, NW., Lower Level, Washington, DC 20555-0001

2. The Superintendent of Documents, U.S. Government Printing Office, P. O. Box 37082, Washington, DC 20402-9328

3. The National Technical Information Service, Springfield, VA 22161-0002

Although the listing that follows represents the majority of documents cited in NRC publications, it is not intended to be exhaustive.

Referenced documents available for inspection and copying for a fee from the NRC Public Document Room include NRC correspondence and internal NRC memoranda; NRC bulletins, circulars, information notices, inspection and investigation notices; licensee event reports; vendor reports and correspondence; Commission papers; and applicant and licensee documents and correspondence.

The following documents in the NUREG series are available for purchase from the Government Printing Office: formal NRC staff and contractor reports, NRC-sponsored conference proceedings, international agreement reports, grantee reports, and NRC booklets and brochures. Also available are regulatory guides, NRC regulations in the *Code of Federal Regulations,* and *Nuclear Regulatory Commission Issuances*.

Documents available from the National Technical Information Service include NUREG-series reports and technical reports prepared by other Federal agencies and reports prepared by the Atomic Energy Commission, forerunner agency to the Nuclear Regulatory Commission.

Documents available from public and special technical libraries include all open literature items, such as books, journal articles, and transactions. *Federal Register* notices, Federal and State legislation, and congressional reports can usually be obtained from these libraries.

Documents such as theses, dissertations, foreign reports and translations, and non-NRC conference proceedings are available for purchase from the organization sponsoring the publication cited.

Single copies of NRC draft reports are available free, to the extent of supply, upon written request to the Office of Administration, Distribution and Mail Services Section, U.S. Nuclear Regulatory Commission, Washington, DC 20555-0001.

Copies of industry codes and standards used in a substantive manner in the NRC regulatory process are maintained at the NRC Library, Two White Flint North, 11545 Rockville Pike, Rockville, MD 20852-2738, for use by the public. Codes and standards are usually copyrighted and may be purchased from the originating organization or, if they are American National Standards, from the American National Standards Institute, 1430 Broadway, New York, NY 10018-3308.

NUREG/CR-6411
PNL-10866

A Geostatistical Methodology to Assess the Accuracy of Unsaturated Flow Models

Manuscript Completed: March 1996
Date Published: April 1996

Prepared by
J. L. Smoot, R. E. Williams*

Pacific Northwest National Laboratory
Richland, WA 99352

T. Nicholson, NRC Project Manager

Prepared for
Division of Regulatory Applications
Office of Nuclear Regulatory Research
U.S. Nuclear Regulatory Commission
Washington, DC 20555-0001
NRC Job Code L2466

*University of Idaho
Geology Department
Moscow, ID 83843

For sale by the U.S. Government Printing Office
Superintendent of Documents, Mail Stop: SSOP, Washington, DC 20402-9328
ISBN 0-16-048648-3

Abstract

The Pacific Northwest National Laboratory (PNNL) has developed a Hydrologic Evaluation Methodology (HEM) to assist the U.S. Nuclear Regulatory Commission in evaluating the potential that infiltrating meteoric water will produce leachate at commercial low-level radioactive waste disposal sites. Two key issues are raised in the HEM: 1) evaluation of mathematical models that predict facility performance, and 2) estimation of the uncertainty associated with these mathematical model predictions. The technical objective of this research is to adapt geostatistical tools commonly used for model parameter estimation to the problem of estimating the spatial distribution of the dependent variable to be calculated by the model. To fulfill this objective, a database describing the spatiotemporal movement of water injected into unsaturated sediments at the Hanford Site in Washington State was used to develop a new method for evaluating mathematical model predictions. Measured water content data were interpolated geostatistically to a 16 x 16 x 36 grid at several time intervals. Then a mathematical model was used to predict water content at the same grid locations at the selected times. Node-by-node comparison of the mathematical model predictions with the geostatistically interpolated values was conducted. The method facilitates a complete accounting and categorization of model error at every node. The comparison suggests that model results generally are within measurement error. The worst model error occurs in silt lenses and is in excess of measurement error.

Contents

Figures

Tables

Executive Summary

The Pacific Northwest National Laboratory (PNNL) has developed a Hydrologic Evaluation Methodology (HEM) for characterizing water movement through the unsaturated zone such as that which occurs at commercial low-level radioactive waste (LLW) disposal sites. The HEM is designed to focus on key technical issues that define the interaction between infiltrating meteoric water and buried waste at LLW disposal facilities. The purpose of this report is to describe a new method that addresses two key issues raised in the HEM: 1) Evaluation of mathematical models that predict facility performance; and 2) Estimation of the uncertainty in mathematically predicted facility performance.

The objective of this research is to adapt geostatistical tools commonly used for model parameter estimation to the problem of estimating the spatial distribution of the dependent variable to be calculated by the model. To fulfill this objective, an existing water content database from an injection test in the unsaturated zone at the Hanford Site in Washington State was utilized (Fayer et al. 1993). The database consists of a comprehensive series of spatiotemporal water content measurements that track the spread of injected water and tracers through an 18-m-thick section of unsaturated sediments via 32 monitoring wells within an 8-m radius.

Evaluation of a transient, three-dimensional mathematical model simulation of water movement in the unsaturated zone is described in this report. The model incorporates a hydrogeologic conceptual model. Measured data and geostatistical estimates of these data are used to develop target values of the dependent variable, volumetric water content, at each model node. Model reliability is investigated by comparing the output at each node to the target value. In summary, the study consists of geostatistical interpretation of this water-content database and development of a three-dimensional unsaturated zone model to predict these water contents using the Subsurface Transport Over Multiple Phases (STOMP) code.

Geostatistical and mathematical model calculations are conducted on a common, uniform, three-dimensional grid. Each grid cell measures 0.9 x 0.9 x 0.5 m, with a total array of 16 x 16 x 36 in the x, y, and z directions, respectively. Water-content data are interpolated on to this grid by (1) development of a global variogram and kriging of the seven different sediment types and by (2) application of a biharmonic cubic spline technique. The resulting matrix with values at each node constitutes a geostatistical database. Node-by-node comparisons between the mathematical model output and the geostatistical database are conducted on the common grid. The a priori model acceptance criterion was to have modeled volumetric water contents within the ±2-3% calibration error of the neutron probes used to collect the field data.

Analysis of simulated water contents indicates that model results generally are within measurement error. The worst model error is determined to occur in silt lenses. The node-by-node analysis approach is recommended for model output evaluation because the geostatistical database facilitates a complete accounting and categorization of model error.

The general conclusion of this study is that use of the geostatistical database significantly improves the ability to check the accuracy of model output. If mathematical model results are to be a cornerstone of regulatory decision making, the study results show that data collection must be balanced between the independent variables that define model input and dependent variables that define model output in the geostatistical database. These data should be collected at a scale sufficient to define them on the common grid. The method allows detailed error analysis of the dependent hydrologic variable; the error then can be analyzed spatially by sector or lithology.

Acknowledgements

This research was supported by Associated Western Universities, Inc., Northwest Division (AWU NW) under Grant DE-FG06-89ER-75522, DE-FG07-93ER-75912 and DE-FG06-92RL-12451 with the U.S. Department of Energy. This research was conducted during a DOE/AWU NW fellowship at Pacific Northwest National Laboratory (PNNL) while the lead author was a Ph.D. candidate at the University of Idaho. PNNL is operated for the U.S. Department of Energy by Battelle Memorial Institute under Contract DE-AC06-76RLO 1830.

Funding for the fellowship was obtained through the U.S. Nuclear Regulatory Commission (NRC JCN L2466) and the U.S. Department of Energy. The authors would like to acknowledge Martin Smith and Renhao Li of the University of Idaho for their guidance with the geostatistical analysis and kriging. Thanks to reviewers Glendon Gee of Pacific Northwest National Laboratory; Dale Ralston, Jim Osiensky, Dennis Horn, and Stan Miller of the University of Idaho; and to Allen Lu of Westinghouse Hanford Company.

Foreword

This technical report was prepared by Pacific Northwest National Laboratory[1] under its research project with the waste management branch in the Office of Nuclear Regulatory Research (JOB CODE L2466). The report presents a geostatistical approach for modeling water content in unsaturated, sedimentary, lithologic units that may be important to assessing ground-water flow and transport at commercial low-level radioactive waste (LLW) sites. This report builds on information and experimental data presented in NUREG/CR-5996: "Subsurface Injection of Radioactive Tracers: Field Experiment for Model Validation Testing" and borehole geophysical logging results reported in PNL-10860 "Re-Evaluation of a Subsurface Injection Experiment for Testing Flow and Transport Models." Specific information is provided on methods to characterize and represent the spatial variability of hydrogeologic units (e.g., unsaturated alluvial deposits) by integrating a geologic conceptual (e.g., fluvial depositional) model, drilling logs and samples, and borehole geophysical logs. Also presented are transient numerical modeling results of the water content distributions in these unsaturated alluvial deposits by incorporating the spatial variability characteristics of the different hydrogeologic units within the deposit. The methods and analyses discussed resolve selected issues associated with site characterization, data collection optimization, and assessment of model accuracy.

NUREG/CR-6411 is not a substitute for NRC regulations, and compliance is not required. The approaches and/or methods described in this NUREG/CR are provided for information only. Publication of this report does not necessarily constitute NRC approval or agreement with the information contained herein.

[1] Pacific Northwest National Laboratory is operated for the U.S. Department of Energy by Battelle Memorial Institute under Contract DE-AC06-76RLO 1830.

1.0 Introduction

1.1 Statement of the Problem

A primary problem in mathematical modeling is developing a system for comprehensive evaluation of modeling results. Development of a mathematical model grid typically results in hundreds or thousands of nodes that form the computational matrix; typical hydrologic sampling networks result in measured values for less than 10% of the nodes. Solution of this data distribution problem, subject to some minimum data requirements, would increase the ability to evaluate mathematical models and allow for quantification of the uncertainty in mathematical predictions.

The Pacific Northwest National Laboratory (PNNL) has developed a Hydrologic Evaluation Methodology (HEM) for characterizing water movement through the unsaturated zone at commercial low-level radioactive waste (LLW) disposal sites. The analytical methodology is designed to focus on key technical issues that define the interaction between infiltrating meteoric water and buried waste at LLW disposal facilities. Two key issues are addressed in the HEM:

1) Evaluation of mathematical models that predict facility performance; and
2) Estimation of the uncertainty in mathematically predicted facility performance.

The purpose of this report is to investigate mathematical techniques that address these issues. To conduct these investigations, an existing database from an injection test site in the unsaturated zone at the Hanford Site in Washington State was utilized. The experiment was reported by Sisson and Lu (1984) and was reviewed extensively in a report prepared for the U.S. Nuclear Regulatory Commission by Fayer et al. (1993). Briefly, the database consists of a series of geophysical measurements that track the spread of serial injections of water containing radioactive tracers through steel-cased observation wells. This study focuses on the movement of water and the ability of a mathematical model to predict this movement.

1.2 Purpose and Objectives

The purpose of this research is to develop and demonstrate a geostatistical approach to document model prediction accuracy by utilizing data from an injection test in the unsaturated zone. The general objective is to develop a geostatistical database, honoring the spatial dependence structure of the geologic conceptual model. The geostatistical database will have an estimated or measured value at every node and is used to evaluate the accuracy of mathematical model output. Model input is based on site characterization data; model output consisting of transient water contents in three dimensions is compared to a transient geostatistical database constructed from field-measured water contents. The method is distinguished by incorporating geostatistics into the analysis of model output rather than the parameterization of model input.

1.3 Method of Study

A previous field experiment is used in this study to develop a geostatistical approach to model validation (Sisson and Lu 1984, Fayer et al. 1993). The experiment consisted of an injection test in the unsaturated zone with a central injection well and 32 monitoring wells. The investigators measured the movement of repeated injections of water and tracers via the monitoring well network. These data were collected for the purpose of testing numerical models of subsurface flow and transport and are well documented in the investigator's 1984 report. Their report includes some preliminary two-dimensional modeling.

The primary rationale for conducting the injection test experiment was to develop a data set that could be used to test mathematical

models of subsurface flow and transport in the unsaturated zone. Research for the current study focuses on development of a geostatistical database to test model output as an approach to model validation. The unique features of the database are the sufficiently complete record of site characterization for model parameterization combined with detailed, three-dimensional, transient monitoring of the dependent variable, water content for injected fluid pulses, that can be compared directly to model output. This detailed monitoring of water content allows the transient response of a site model to be checked very precisely.

These data provide a good opportunity for model testing because there is sufficient data for both mathematical model parameterization and independent evaluation of model output. Geologic and hydrologic data from the site characterization database (Sisson and Lu 1984, Fayer et al. 1993, Smoot 1995) are analyzed in three dimensions for this study to develop a geologic conceptual model and subsequently parameterize model input. A wide range of separation distances exists between the monitoring wells, suggesting that the site is well adapted for understanding the spatial correlation in these data via geostatistical analysis. Geostatistical techniques are used to analyze the fluid migration data, collected as water content, at selected times from the monitoring wells for the purpose of analyzing model output. These data are kriged onto a nodal grid with the same dimensions and spatial coordinates as the mathematical model grid. These data also are interpolated to the same grid using a biharmonic cubic spline technique. The spatial data analysis techniques of kriging and splines are used to augment the high-quality field database to build a gridded matrix of measured data and estimated values, incorporating the spatial dependence structure to test a model developed for the site. The approach results in a geostatistical database consisting of a full matrix of target values in one-to-one correspondence with the nodes forming the matrix of the model output grid.

Evaluation of model output consists of calculation of differences (errors) at each node between the geostatistical database and the model output. Error at each node is grouped based on several spatial categories, and statistics are calculated for each category after a complete sweep of the grid. The method categorizes model accuracy by spatial subregions in terms of compass heading, depth, and lithology.

Smoot (1995) extensively reviewed the problem of model validation and evaluating model output. A number of authors discuss the pros and cons of model validation (Tsang 1991, Larsson 1992, Bredehoeft and Konikow 1993, Bair 1994, McCombie and McKinley 1993, Oreskes et al. 1994). Wang and Williams (1984) accurately pointed out that a knowledgeable regulator must ultimately defend some position based on available information, including predictions and answers provided by models.

Such model predictions for subsurface processes constitute a spatial distribution of the dependent variable that commonly is evaluated at selected locations where measurements exist. However, measurements usually exist at only a few percent of the total number of nodes in a model grid. Therefore, exploitation of the spatial dependence structure provides a physically based method to estimate the values at unmeasured locations (nodes) using the concepts of geostatistics.

Delhomme (1978) described the utility of kriging and its potential for parameter estimation, automatic contouring, and measurement network design. He was one of the first to point out the potential for kriging to guide the selection of model parameters during calibration. Neuman and coworkers also noted the utility of kriging for parameter estimation, particularly in the context of inverse calibrations of ground-water flow models (Neuman 1980, Neuman 1982, Neuman 1984, Neuman et al. 1980, Neuman and Yakowitz 1979). Commonly, these geostatistical applications are incorporated into probabilistic and/or stochastic methods. Neuman (1982) discussed statistical characterization of aquifer heterogeneity. He also discussed stochastic

methods, including kriging and conditional simulation of transmissivity data. Zirschky (1985) reviewed the kriging technique and described its potential for environmental applications. Gilbert and Simpson (1985) and Cooper and Istok (1988) reviewed basic geostatistics and their application in contaminant hydrogeology.

Rockhold et al. (1994) described a deterministic method for conditioning the hydraulic properties needed to parameterize unsaturated zone model input. The conditioning is based on the spatial distribution of initial water content and calculated scale-mean hydraulic parameters. Reasonable matches to observed data were obtained without calibration, suggesting an alternate approach to stochastic methods for studying spatial variability.

Neuman and coworkers have utilized the concept of node-by-node analysis in the development of a statistical approach for transmissivity estimation in the inverse problem. Neuman and Yakowitz (1979) and Neuman (1980) used a comparative analysis of model results with a theoretical "known" transmissivity distribution to select a solution to the problem. They used statistical measures, including mean residual sum of squares and average residual, to analyze the results. The analysis was not conditioned based on any hydrogeologic knowledge of the aquifer; all transmissivity points were assumed to be from the same population. Neuman (1980) calculated the actual error based on a known theoretical distribution of transmissivity, but noted that in practice the actual distribution is not known.

Evaluation of geostatistical techniques suggests that a physically based model of the spatial dependence structure can be developed using geostatistics. Consequently, development of a defensible array of target mathematical model output values by utilizing the measured data and the spatial dependence structure theoretically is tractable. Development of these target values into a geostatistical database and use of this database to check model output is the subject of this report.

2.0 Geologic Conceptual Model

2.1 Introduction

A geologic conceptual model for the injection test site is described in this section. The geography and layout of the site are described by Fayer et al. (1993) and Smoot (1995). The location of the study area is shown in Figure 1. The site originally was chosen by Sisson and Lu (1984) because geologic reconnaissance suggested simple geology and relatively homogeneous, sandy alluvium. An injection well and 32 monitoring wells were drilled (Figure 2). Evaluation of the drilling and geophysical logs from these boreholes indicates that the geology is more complex, consisting of layers and lenses of finer and coarser alluvial sediments.

2.2 Geology of Surficial Sediments

The geology at the Hanford Site consists of the Miocene Columbia River Basalt Group overlain by late Miocene-Pliocene Ringold Formation and the Pleistocene Hanford Formation. The sediments of the Ringold Formation disconformably overlie the Columbia River Basalt Group over much of the site, including the southern two thirds of the 200 East Area. The Hanford Formation sediments overly the Ringold Formation; a small portion of the Hanford Formation sediments were analyzed for this study.

Deposition of sediments at the Hanford Site has been extensively studied. Most evidence suggests that the sediments at the injection test site were deposited by a series of catastrophic floods from Pleistocene Glacial Lake Missoula. Waitt (1984) reported on the periodicity of these floods. Evidence from northern Idaho and Washington corroborates evidence from southeastern Washington that one graded bed was deposited per flood. Fourteen sets of alternating varved mud and sand similar to the southeastern Washington slackwater deposits are observed in the Priest Lake valley, while a succession of at least 28 flood beds is observed near Spokane.

Mullineaux et al. (1978) discussed the age of the most recent catastrophic flood that would have deposited all or part of the sediments at the injection test site. They correlated Mount St. Helens pumice (set S) with certain ash beds associated with young flood deposits of the channeled scablands. The correlation suggests an age of about 13,000 ^{14}C yr B.P. for the last major flood to have crossed the scabland compared to the previous estimate of approximately 20,000 yr B.P.

Hanford Formation sediments range from fine-grained silts to coarse-grained gravel, cobbles, and boulders. The distribution of these materials deposited at any specific location depended on the energy levels of each flood and proximity to main flood channels. These concepts form the foundation for a conceptual model: a series of fining-upward sedimentary sequences deposited by successive catastrophic floods. However, the simple model is complicated by reworking of the uppermost fine material during each hiatus and probable removal of portions of the material by the subsequent flood.

Drilling logs from 32 wells at the injection test site (Smoot 1995) suggest the following lithology. The upper 1.5 m is a moist coarse sand underlain by approximately 4.6 m of fine sand with some clay. This unit tends to coarsen to the west and locally appears to be coarser near the center of the site. A 6-m-thick unit with mixed fine-grained and coarse-grained material in approximately a 2:1 ratio underlies this unit on the west side of the site. In the center of the site, the unit appears to thin to approximately 3 m of very fine sand with 10% clay-sized material. The remainder of the material at depth is described in most well logs as a coarse sand with varying amounts of gravel and occasional reports of a clay-sized fraction. However, 6 m of fine sand

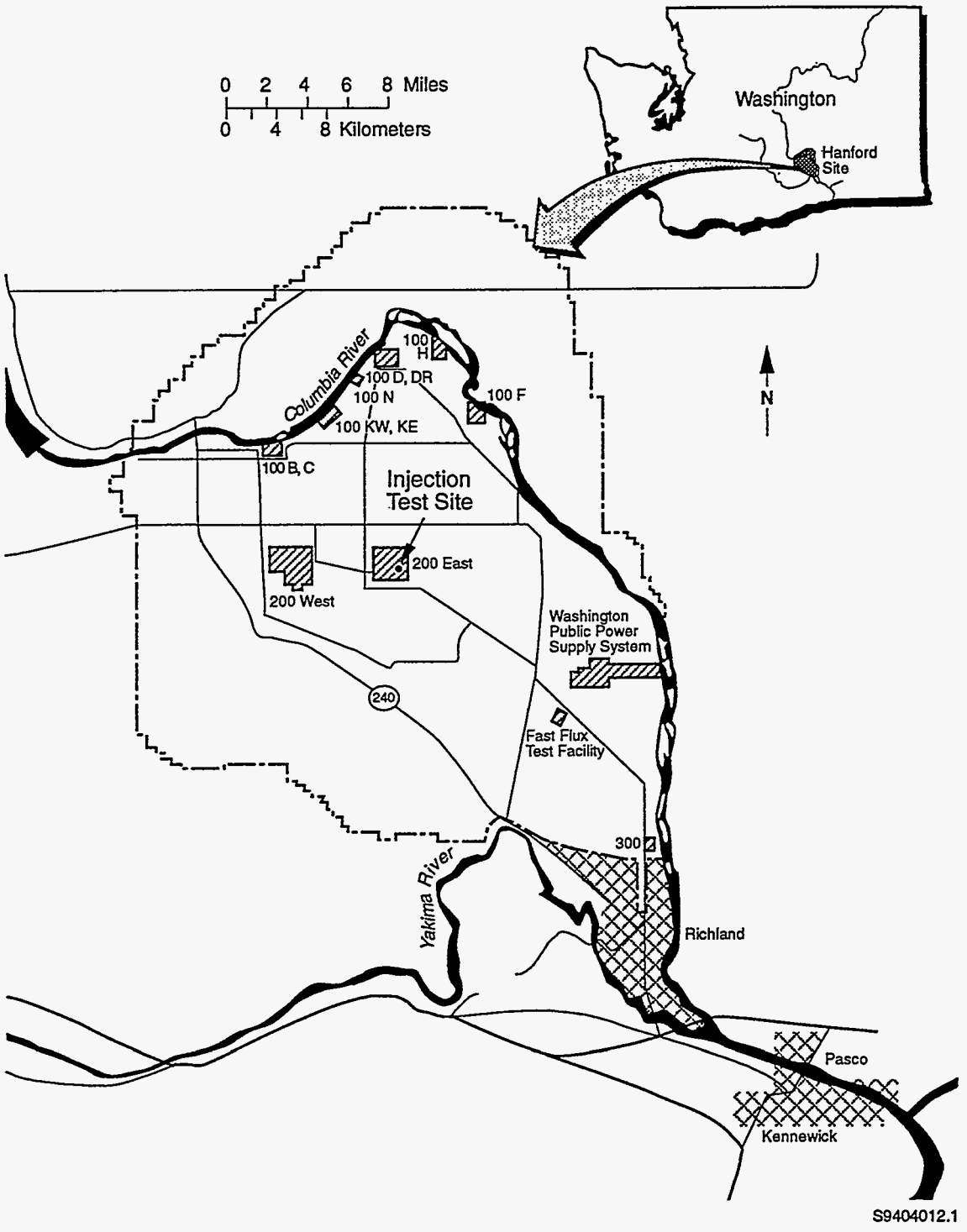

Figure 1. Location of injection test site

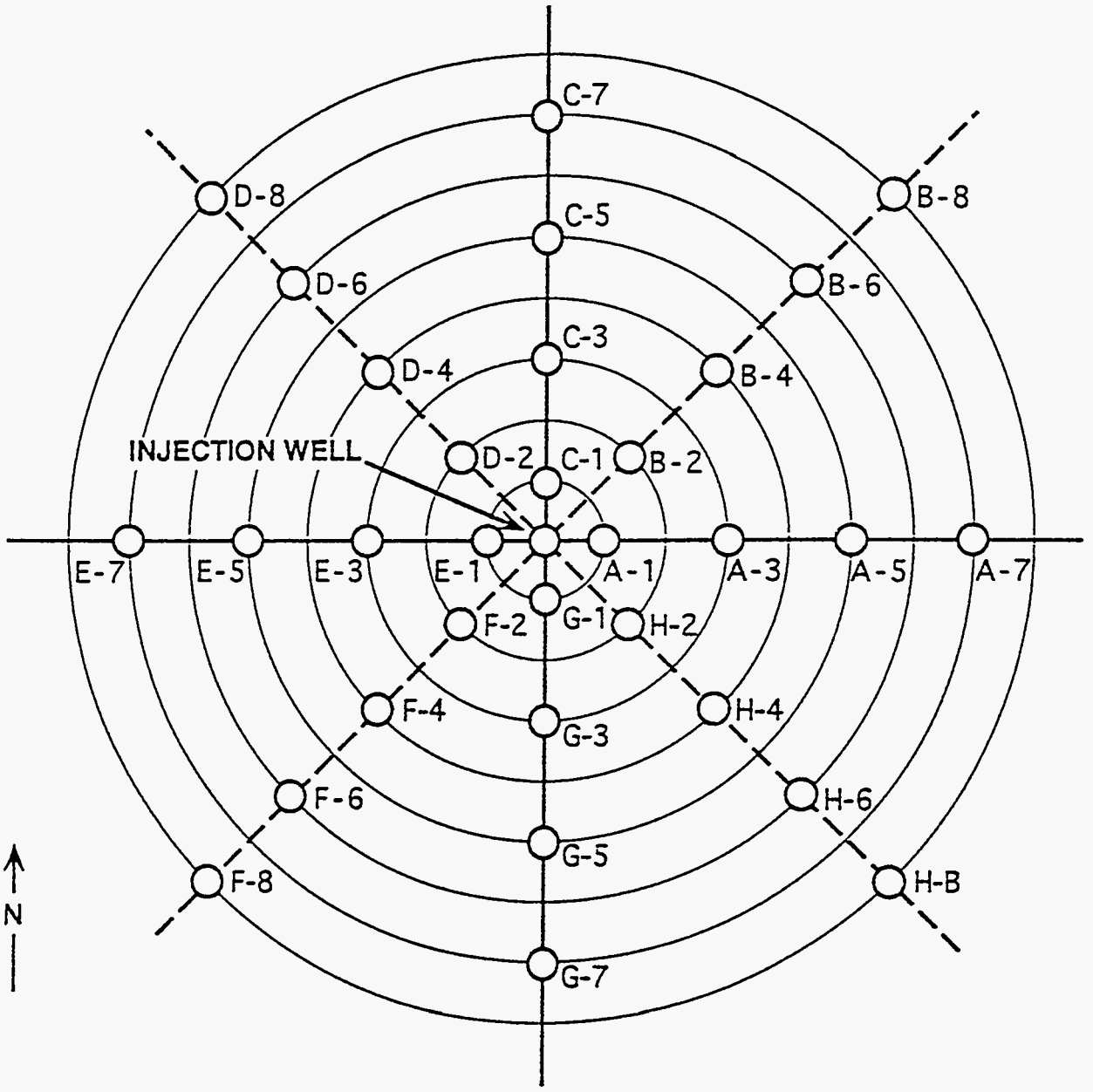

Figure 2. Well array at injection test site

constitutes the lowest reported interval in the northwest part of the site.

From three of the observation wells, sediment samples were collected every 1.5 m or at smaller intervals if a major change in lithology was encountered. Samples were not collected from any other wells. Nineteen of these samples constituting a representative range of soil types were tested in a laboratory to determine physical and hydraulic properties, including particle density, size distribution, and saturated hydraulic conductivity (Sisson and Lu 1984, Fayer et al. 1993). Pressure plate and vapor adsorption data were measured for all samples; hanging-water-column data were measured for eight of the samples.

2.3 Geophysical Logging

Neutron, natural gamma, and gamma-gamma logging were conducted by Sisson and Lu (1984) as part of the original experiment. In a related investigation (Fayer et al. 1995), Schlumberger, Inc. logged all of the observation wells in January 1995, using state-of-the-art sondes that have been adapted from oil- and gas-well logging for use in environmental monitoring wells. Their logging included complete passes of the observation well network using a compensated neutron sonde, a litho-density sonde, and an accelerator-porosity sonde.

Sisson and Lu measured water-content values versus depth in the observation wells with three Campbell-Pacific Nuclear (CPN) neutron probes (Fayer et al. 1993). Schlumberger, Inc. used a Compensated Neutron Sonde (CNT-G) and an Accelerator Porosity Sonde (APS) for neutron logging. The CNT-G operates on the same principle as a neutron probe to measure the presence of the hydrogen atom. Where the hydrogen concentration of the formation is large, most of the neutrons are slowed and captured within a short distance of the source. On the other hand, if the hydrogen content is low, more of the neutrons will travel farther before they are captured. The CNT-G detects the presence of hydrogen by counting epithermal neutrons--the more neutrons, the lower the hydrogen content.

Both gamma-ray and gamma-gamma logging were conducted at the site. The gamma-ray log measures the natural radioactivity of the formation and typically is a measure of shale or clay content which tend to contain radioactive elements. The gamma-gamma log measures the electron density of the formation. The tool irradiates the formation with medium-energy gamma rays that collide with electrons in the formation. At each collision, a gamma ray loses some, but not all, of its energy to electrons, and continues with diminished energy. The scattered gamma rays reaching the detector on the sonde, at a fixed distance from the source, are counted as an indication of formation density, hence porosity. The Litho-Density Sonde (LDS) used by Schlumberger, Inc. has dual detectors that allow the tool to correct for borehole effects. This tool also measures the photoelectric absorption index for the formation. This index can be related to lithology; whereas, the bulk density measurement responds primarily to porosity.

An interpretation of the gross gamma response for Schlumberger's CNT-G log is shown in Figure 3. This figure shows a cross section through the principal east-west axis of the site. The cross-section is a slice from a three-dimensional interpretation derived from a cubic spline algorithm that incorporates the gamma response from all 32 monitoring wells. Elevated gamma levels (red and orange zone) in well E-1 just west of the injection point (INJ) are attributed to residual levels of ^{134}Cs utilized as a tracer during the experiment. Several orange zones are also observed at depth below the injection point.

The matrix bulk density for Schlumberger's LDS log on the same section line is shown in Figure 4. Again, bulk density values are interpolated to this section using a cubic spline algorithm that incorporates the response from all 32 wells. The matrix bulk density response shows distinct layering, with the warmer

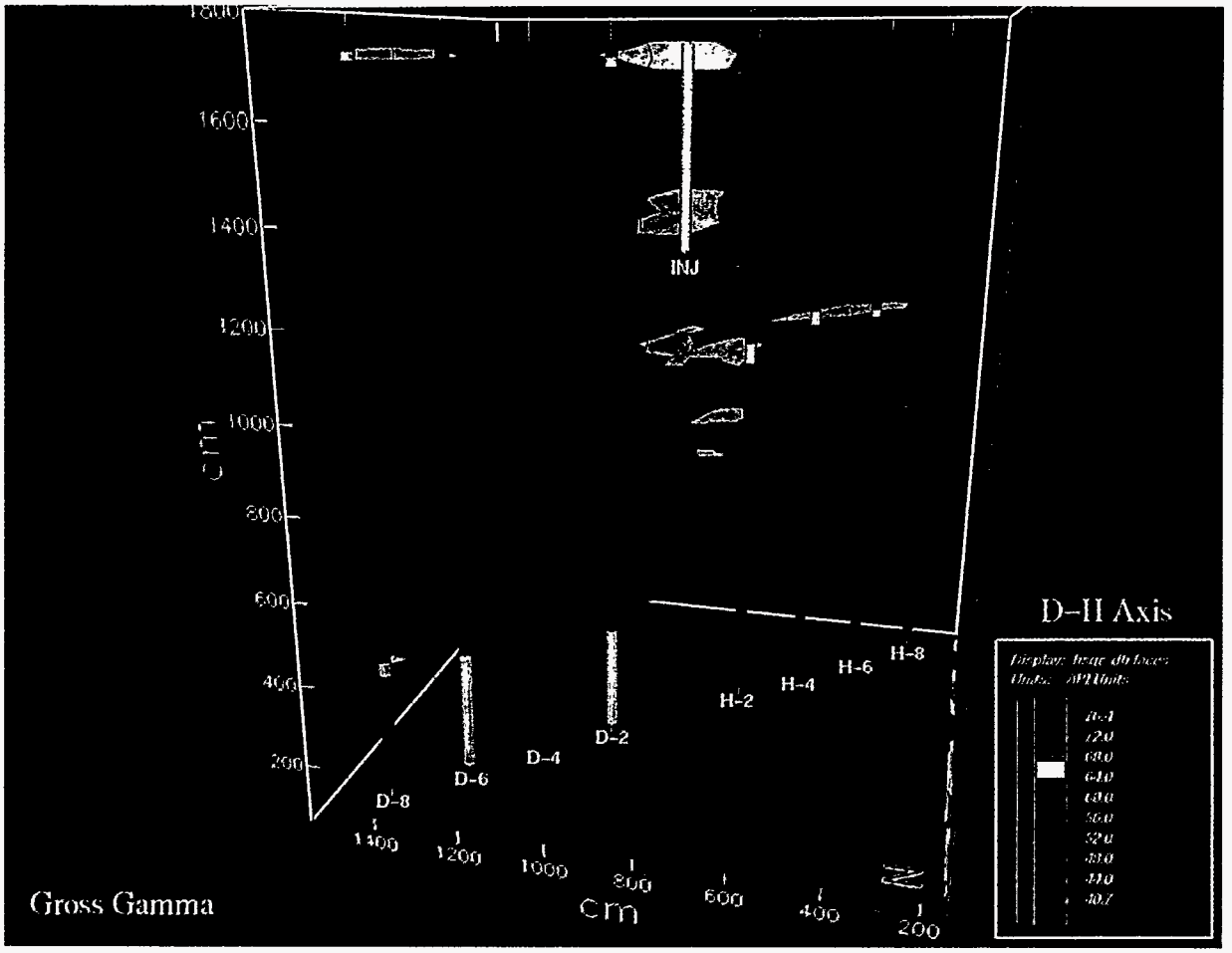

Figure 3. Gross gamma response for Schlumberger's CNT-G log

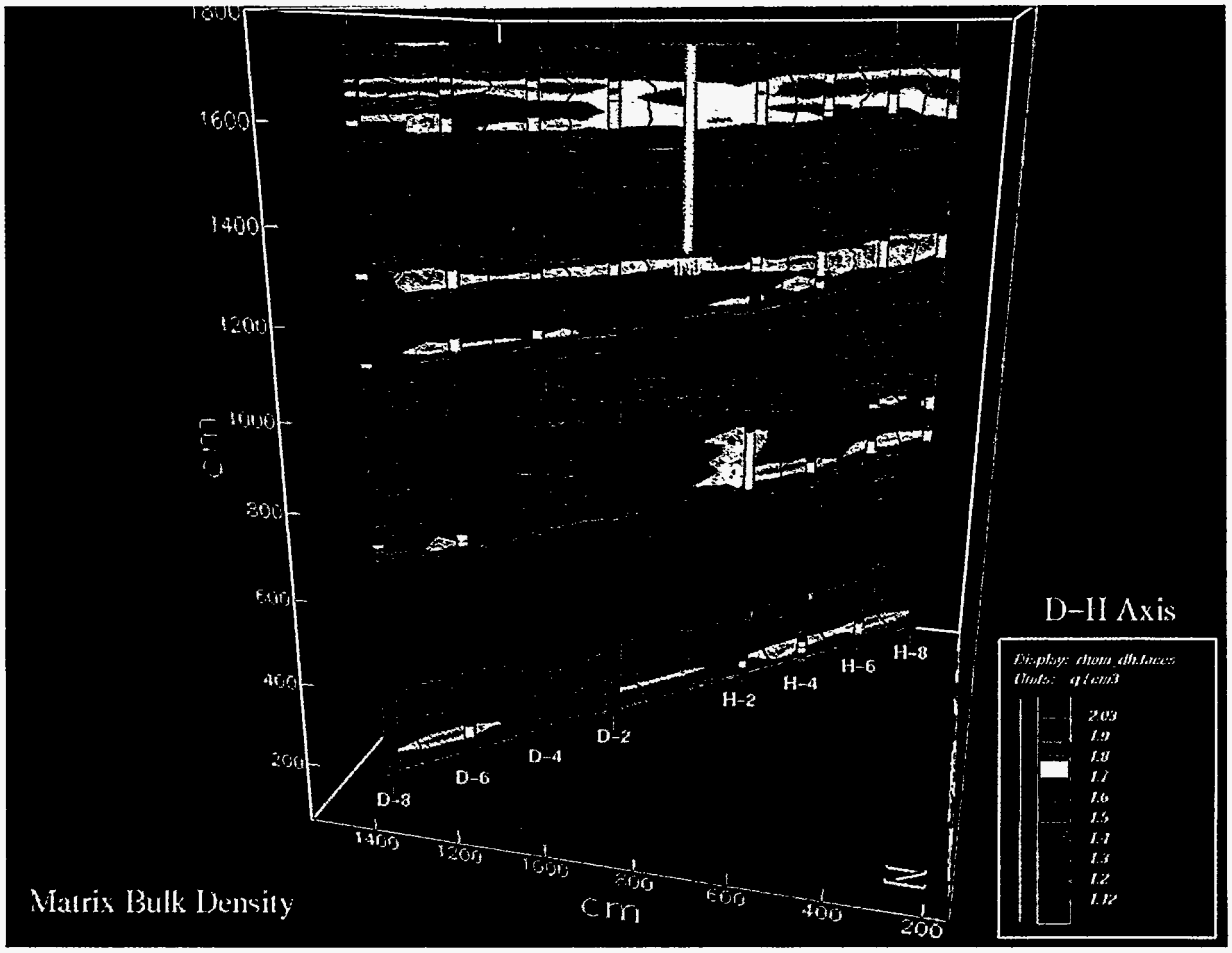

Figure 4. Matrix bulk density response for Schlumberger's LDS log

yellows, oranges, and reds (lighter tones) representing layers of higher bulk density and the blues, greens, and purples (darker tones) representing layers of lower bulk density.

2.4 Interpretation of Lithology

Lindsey[1] interpreted the stratigraphy of the site based on drilling logs, published information for the 200 East Area, and years of experience conceptualizing stratigraphy in the flood deposits. His interpretation indicated approximately seven sediment types. These sediment types and their abbreviations are summarized in Table 1. These sediments consist of wedges and lenses of alternating coarser and finer sediments located within a matrix of medium to coarse sand. The coarser sediment is labeled as coarse sand to gravel; several fine-grained sediments are noted also. These fine-grained sediments include a silty to medium sand, a silty fine to medium sand, silty sand to silt, and silt. Some layers are not continuous, and some of the fine-grained layers occur as lenses. Therefore, the site is heterogeneous, with both continuous and discontinuous layers.

Table 1. Sediment types identified at test site

Sediment Type	Abbreviation
Silt	silt
Silty, fine to medium sand	sfms
Silty to medium sand	ssms
Medium to coarse sand	mscs
Medium sand to gravel	msgr
Coarse sand to gravel	csgr
Interbedded medium-to-coarse sand and gravel	mcgi

Five textural changes are observed vertically in the sediment, based on study of the drilling logs and incorporation of the work of Lindsey[1]. These five textural changes, with approximate depth intervals, may be summarized as follows. The upper layer (0 to 300 cm) consists of silty fine- to medium-grained sand, occasionally overlain by coarser sediments. The silty sediments may be interbedded or mixed. The second layer (301 to 600 cm) consists of medium- to coarse-grained sand. The third layer (601 to 1200 cm) contains lenses of silt and gravel within medium- to coarse-grained sand. The fourth layer (1201 to 1600 cm) consists predominantly of coarse-grained sand with interbedded gravel. The fifth layer (1601 to 1800 cm) is somewhat finer, with fine- to coarse-grained sand with minor interbedded silt.

These textural changes appear broadly to be consistent with the average gamma-gamma response across the site (Figure 3). The textural changes indicate alternating layers of coarser- and fine-grained material. Consequently, the fine-grained layers would be expected to retain more water than the coarse-grained layers, resulting in an alternating pattern of higher and lower gamma-gamma response as observed in Figure 3.

1. K. A. Lindsey, 1994. Personal communication.

3.0 Codevelopment of Target Database and Mathematical Model

3.1 Introduction

In order to improve the model evaluation process, unsaturated zone water content data collected periodically from the suite of observation wells (Sisson and Lu 1984, Fayer et al. 1993) was interpolated to a regular grid in three-dimensional space. Concurrently, a mathematical model to predict these measured water content data was developed using the same grid. This section describes the common grid, development of the geostatistical target database, and the construction of the mathematical model. Detailed discussion of the development is contained in Smoot (1995).

3.2 Gridding of Subsurface Geologic Units

The subsurface zone of investigation is a rectangular prism that incorporates the zone of measurement at the injection test site. The surface area may be approximated as a square with edge length of approximately 14.5 m. The depth is 18 m that includes the maximum depth of neutron probe measurements in the observation wells.

The model domain is discretized into rectangular prismatic cells that measure 0.9 x 0.9 m in the horizontal plane and 0.5 m in the vertical plane. The cell structure is 16 x 16 x 36 for a total of 9216 cells. The vertical dimension is half the horizontal dimension to account for the dominant horizontal extent of the lithologic units. In addition, field measurements indicate that 0.5 m is a reasonable minimum length to account for field-scale geologic and water content heterogeneity that were described in Section 2.

Seven different lithologies are listed in Table 2. Each cell in the model was identified uniquely with a lithologic type based on three-dimensional interpretation of the extent of the geologic units. Groups of cells of the same lithology form the geometric arrangement of the layers, wedges, and lenses of sediment present at the site. The distribution of cells by lithologic type is shown in Table 2.

The three-dimensional model was constructed using minimum curvature algorithms with contact information described for each borehole. Five textural changes are observed vertically with depth in the sediment. The upper layer (0-3 m) consists of silty fine- to medium-grained sand, occasionally overlain by coarser sediments. The silty sediments may be interbedded or mixed. The second layer (3-6 m) consists of medium- to coarse-grained sand. The third layer (6-12 m) contains lenses of silt and gravel within medium- to coarse-grained sand. The fourth layer (12-16 m) consists predominantly of coarse-grained sand with interbedded gravel. The fifth layer (16-18 m) contains fine- to coarse-grained sand and silt.

The three-dimensional nodal distribution of the sediments in the model is shown in Figure 5. The front portion of the block has been cut away to reveal a portion of the interior nodes. The distribution of sediment in the model is derived from the conceptual model of layers, lenses, and wedges of sediment derived from deposition due to successive catastrophic flood deposits. This view shows the orientation of the geologic units exactly as they are input to the model. Cell boundaries show up as blocky features around the perimeter of each unit.

Table 2. Lithology of model cells

Sediment Type	Number of Cells
Silt	41
Silty, fine-to-medium sand	1318
Silty sand to medium sand	287
Medium sand to coarse sand	4220
Medium sand to gravel	124
Coarse sand to gravel	2178
Interbedded medium sand, coarse sand and gravel	1048
	9216

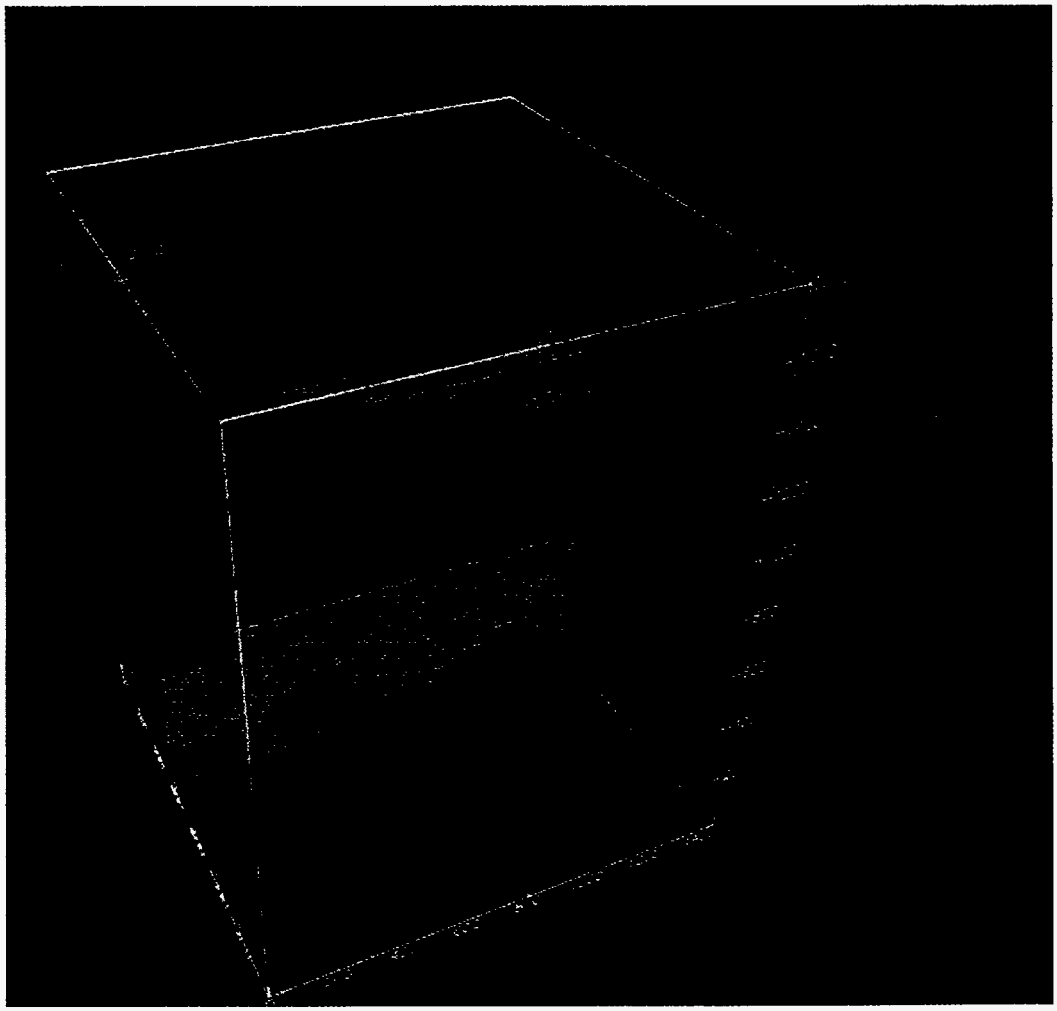

silt	light purple	msgr	light green
sfms	dark purple	csgr	light orange
ssms	blue	mcgi	dark orange
mscs	dark green		

Figure 5. Three-dimensional view of lithology

3.3 Geostatistical Target Database

The geostatistical target database is developed using physically based models for the spatial dependence structure and applied using the technique of kriging to estimate water content values at the unmeasured nodes in the grid. Alternatively, water content values are estimated to the unmeasured nodes using biharmonic cubic splines. As Matheron (1981) has shown, splines and kriging are equivalent techniques in that they are derived from the same mathematical equations.

3.3.1 Spatial Dependence Structure

Measured water content data represent only about 20% of the total volume of sediment tested during the experiment. The unique and desirable characteristic of the geostatistical database is that it contains a value of water content at every location. Therefore, it is necessary to estimate the water content for the unmeasured space between the boreholes. Water contents are estimated for a grid identical to that developed for the mathematical flow model. Two methods are used to estimate the water contents: 1) a kriging algorithm that explicitly considers the spatial dependence structure of the geologic system and 2) a biharmonic cubic-spline algorithm that does not consider explicitly the geologic structure. The methods are evaluated with respect to choosing the best target for conducting node-by-node comparisons with the model results.

An exploratory data analysis was conducted on neutron probe data. Nine time planes were selected for analysis and construction of the geostatistical target database; the first time plane describes the state of the system prior to injection. Eight subsequent time planes were selected at both early and late times relative to selected injections. Reference to these time planes will be abbreviated as tp1, tp2, ..., tp9. There are 1920 data points per time plane. The mean water content initially is 5.4%; it rises to approximately 6.5% during the later time planes. The standard deviation ranges between 2% and 3%; the skewness ranges from 1.4 to 3.3, with all values being positive, indicating moderate to significant right tail in the distributions.

Spikes of high water content are associated primarily with silty fine to medium sand and medium to coarse sand. These sediments consist of finer to intermediate grain-sized material that would be expected to retain this amount of water. The pore-size distribution of coarser sediments would contain a significant increment of larger pore sizes that would not be able to retain the observed quantities of water.

Analysis of water content with respect to soil type indicates that there are significant differences in water content between soil types. Summary statistics for each soil type are listed in Table 3 for tp1. Soils are arranged from finest to coarsest. Consequently, counts theoretically should be in descending order in the tables, but some fluctuations in the pattern are observed. The counts for tp1 range from 426 to 1281 counts (3 to 17% water content). The highest mean counts are 774.8 for ssms and 780.9 for sfms, units with high silt content. After three injections (Smoot 1995), the range for tp4 is 426 to 1564 counts (3 to 21% water content). The highest counts are for fine-grained units with lower counts in the coarse-grained units. The correlation is not perfect. Pure silt is still lower than sfms and ssms but has significantly increased in water content (by 136 counts) after three injections compared to coarse-grained units that generally increased by only several tens of counts.

Table 3. Water count statistics, tp1

Soil	Mean	St. D.	Minimum	Maximum
silt	610.8	127.3	468	919
sfms	780.9	183.4	460	1281
ssms	774.8	169.1	546	1202
mscs	626.0	111.8	448	1236
msgr	545.0	44.6	457	678
csgr	567.5	94.5	426	1098
mcgi	596.4	67.4	472	836

The initial water content (tp1) was analyzed to understand the spatial correlation between water content and the underlying hydrogeologic conceptual model. Geostatistical analyses of neutron probe counts taken prior to the injections are consistent with the lithologic interpretation of the site. These analyses were conducted on raw neutron probe counts to avoid any bias produced by the neutron probe calibration curve used to convert the probe counts to volumetric water contents. All 1920 count locations (60 per observation well) were incorporated into the analysis. The mean probe count for the initial conditions was 630.5 counts/15 s, with a variance of 18,603 (counts/15 s)^2.

The variogram is a spatial moment that describes the average decrease in similarity between pairs of attribute measurements as the separation distance increases. It is calculated as half of the average squared difference in attribute value between points of approximately the same separation distance as (Isaaks and Srivastava 1989):

$$\gamma(h) = \frac{1}{2n}\sum_{i=1}^{n}(x_i - y_i)^2 \quad (1)$$

The experimental variogram consists of the plot of the spatial moment versus the separation distance. The variogram has a range of influence; as the separation distance increases, the value of the variogram increases until the range of influence, or range, is exceeded. Beyond the range, the variogram tends toward a constant value approximately equal to the population variance of the attribute. This constant value is termed the sill. The value of the variogram is 0 if the separation distance is 0. However, short-scale variability and measurement error may cause significant differences for points at short separation distances (Isaaks and Srivastava 1989). Consequently, the value of the variogram may effectively be nonzero at short separation distances. This phenomena is termed the nugget effect.

The experimental variogram is then fit using continuous functions of the form (Isaaks and Srivastava 1989):

$$\gamma(h) = \sum_{i=1}^{n} |w_i|\gamma_i(h) \quad (2)$$

For this study, a summation of nugget and spherical models was used to fit the variogram. The nugget model has the form (Isaaks and Srivastava 1989):

$$\gamma_0(h) = \begin{cases} 0 & \text{if } h = 0; \\ 1 & \text{otherwise} \end{cases} \quad (3)$$

The spherical model has the form (Isaaks and Srivastava 1989):

$$\gamma(h) = \begin{cases} 1.5\frac{h}{a} - 0.5\left(\frac{h}{a}\right)^3 & \text{if } h \leq a; \\ 1 & \text{otherwise} \end{cases} \quad (4)$$

Horizontal and vertical variograms were calculated from these count data to investigate spatial continuity in these two directions. The horizontal variogram (Figure 6) exhibits a reasonable shape but levels off to a sill of approximately 15,000 counts. This is less than the expected value, which should be approximately equal to the sample variance. The vertical variogram (Figure 7) appears to have some average sill in the region of the variance; the variogram exhibits some sinuosity, which suggests a layered system. This is similar behavior to that observed by Desbarats and Bachu (1994), which they attributed to alternating layers of sand and shale. The vertical variogram has a range of 150 to 200 cm, while the horizontal variogram has a range of 300 to 400 cm. These ranges indicate approximately the range of spatial continuity in each direction. The lithologic layers discussed in Section 2 range from 200 to 600 cm in thickness, which is reasonably consistent with the vertical variogram.

The global variogram is shown in Figure 8. The variogram has a sill of approximately

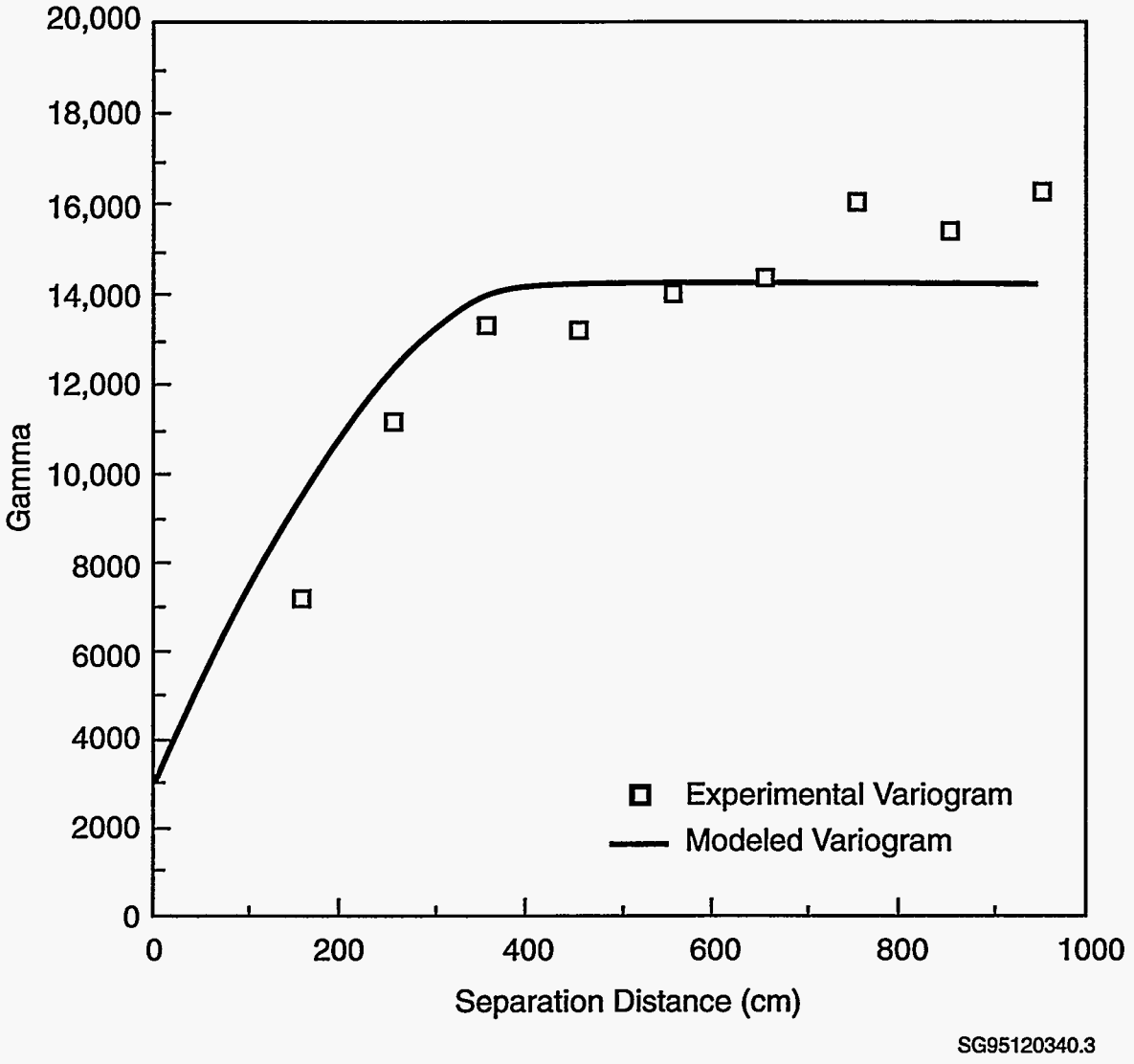

Figure 6. Horizontal variogram of neutron probe counts, initial conditions; model: $g(h) = 3000 + 11000Sph_{375}(h)$

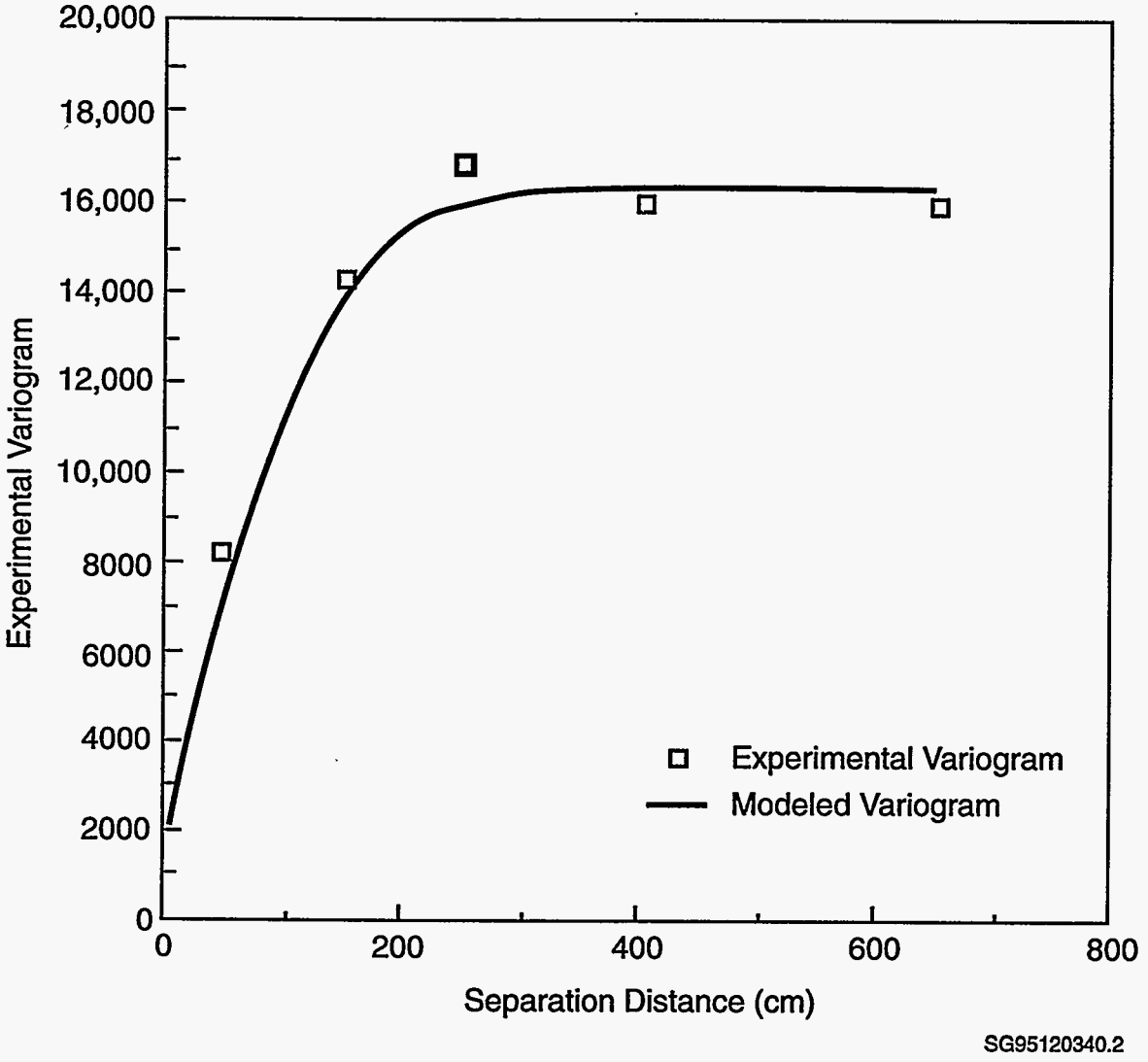

Figure 7. Vertical variogram of neutron probe counts, initial conditions; model: $g(h) = 2000 + 14000Sph_{225}(h)$

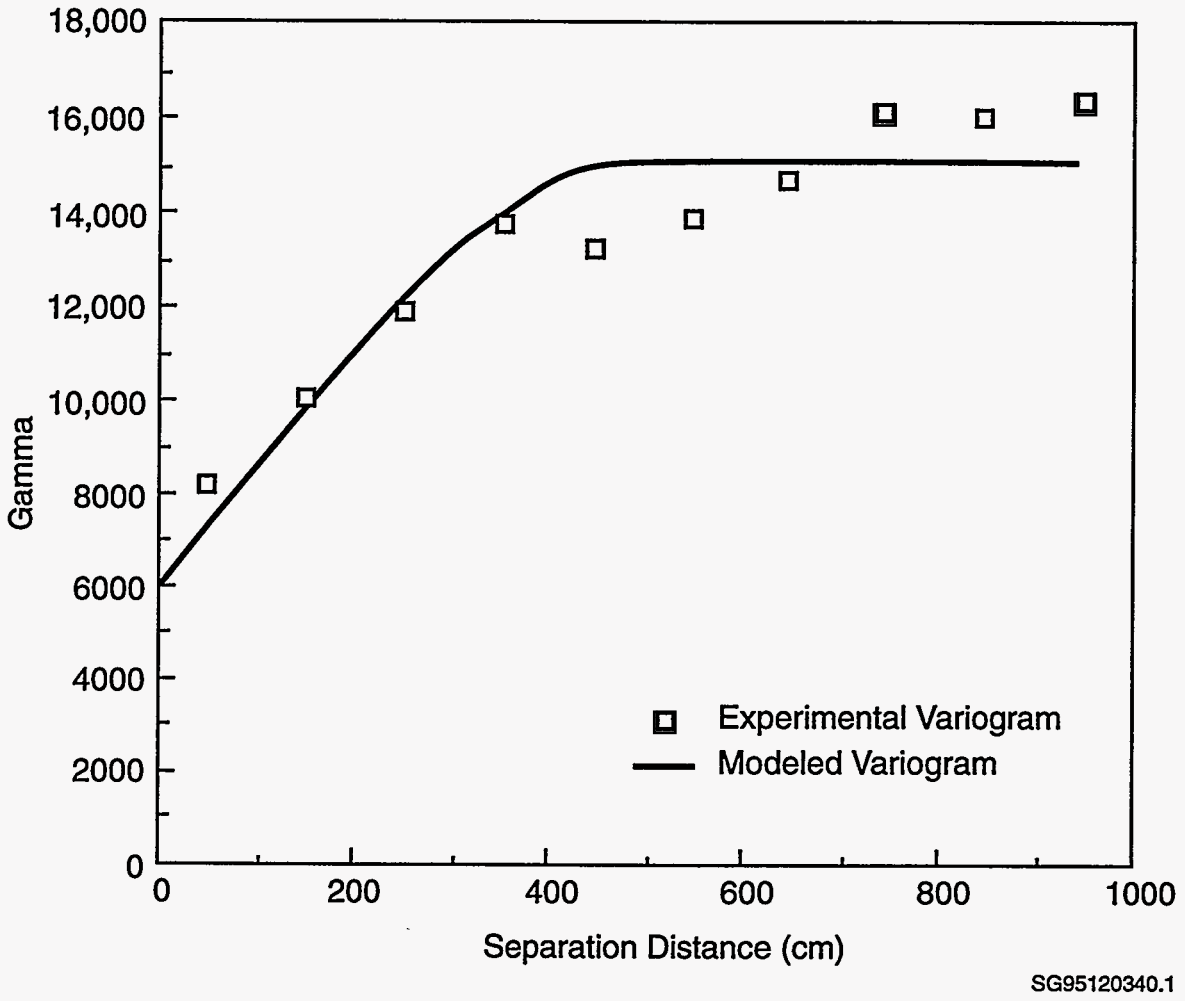

Figure 8. Global variogram of neutron probe counts, initial conditions; model: $g(h) = 6000 + 9000Sph_{500}(h)$

15,000 and a range of approximately 400 cm. The global variogram is estimated using a composite nugget plus spherical model. The parameters of this model are nugget = 6,000, subsill = 9,000, and range = 500. Separate variograms also were calculated for selected soil types using the hydrogeologic conceptual model to subdivide the neutron probe measurements.

Variograms for selected lithologic unit subpopulations were also calculated for a fine-grained unit (sfms), an intermediate unit (mscs), and a coarse-grained unit (mcgi). The variogram for sfms has a range of approximately 75 cm and a sill of approximately 28,000, while the variogram for mscs has a range of approximately 150 cm and a sill of approximately 12000. The vertical and horizontal variograms for mcgi are similar with a range of approximately 250 cm. The horizontal variogram has a well-defined sill at approximately 4500 while the vertical variogram is less distinct at approximately 6000-7000.

The subpopulation variograms suggest differences in the spatial dependence structure among lithologic units. The variograms for these three units exhibit increasing ranges and decreasing sills as texture goes from fine to coarse. The high sill and short range for the sfms indicates significant differences in water content within this unit. This might reflect varying silt content and associated structure within the unit and corresponding changes in water retention characteristics. One lens of this unit is located close to the surface and some of the difference might reflect high water contents near the surface resulting from higher-than-average precipitation during the 6 months preceding the experiment. These factors appear to diminish for the coarser sediments that drain more readily. The sill for mscs is approximately half that of the sfms and the range is approximately doubled. The sills for mcgi are approximately half that of the mscs and the range again is approximately doubled.

3.3.2 Kriging Estimation of Water Content

Water contents first were estimated spatially in the zone of the injection test using the technique of kriging. The conceptual framework for the technique was developed by Krige (1951) and later formalized by Matheron (1963, 1971), who named the technique in honor of Krige's initial efforts. The text by Journel and Huijbregts (1978) and the more recent texts by Isaaks and Srivastava (1989) and Samper and Carrera (1990) review the theory and practice of the method. Current research in three-dimensional geostatistics (Chu, Xu, and Journel 1994) indicates the importance of prior geological information and the incorporation of three-dimensional visualization software (Alexander et al. 1991).

Kriging incorporates the spatial correlation summarized in the variogram and implements a best, linear, unbiased estimate for the spatially continuous variable of interest. The kriging equations are of the form (Isaaks and Srivastava 1989):

$$v_e = \sum_{j=1}^{n} w_j \cdot v_j \qquad (5)$$

$$\sum_{j=1}^{n} w_j = 1 \qquad (6)$$

where v_e is the estimated value, v_j are measured values, and w_j are weights corresponding to each measured value derived from the variogram. The value of the weights sum to 1. In addition, solution of the equation provides an estimate of the error associated with the estimated value.

In this study, kriging is conducted to estimate water contents in the unsampled areas between observation wells. Three methods were investigated: 1) kriging with all water content measurements and the global variogram, 2) kriging each soil type separately with a soil-specific variogram and soil-specific water content measurements, and 3) kriging each soil

type separately with soil-specific water content measurements but using the global variogram for all soils.

The kriging error analysis is shown in Table 4 for all measured points. The error analysis was accomplished by the process of cross validation, also called jackknife kriging. In this method, one measured point is left out of the kriging process and the estimated value is compared to the known value. This process is repeated for the set of measured points and a cumulative error calculated. The mean for the raw data is 630 with a variance of 18,120. Kriging maintains the mean of 630 but reduces the variance to 7486. The reduction in variance would be expected because kriging tends to smooth the extremes during estimation.

Table 4. Kriging error analysis

	n	mean	diff	mse	var
raw	1951	630	0	0	18120
v-all	1951	630	0.1	7367	7486

Smoot (1995) describes kriging error analysis for three of the soil types described in this study. These populations were kriged using soil-specific variograms as well as the global variogram. The mean square error is smaller in all three cases when the population specific variogram for each soil type is used. For mcgi, kriging with its own variogram results in a mean square error of 3175 versus 3901 using the global variogram. For sfms, the soil-specific variogram results in a mean square error of 18426 versus 18989 with the global variogram. For the upper layer of mscs, the corresponding numbers were 8508 and 8741 respectively. The variances on the subpopulations do not show as strong a correlation. For mcgi, the lowest variance is for the subpopulation variogram, while for sfms and the upper layer of mscs, using the global variogram produces a lower variance.

Kriging with the global variogram considering all data from one population results in smoothed estimates of the variable. However, by incorporating information from the hydrogeologic conceptual model, subpopulations based on lithology were identified and kriged locally. Kriging each subpopulation with its own variogram produces the best results. However, only a modest reduction in the mean square error of the estimated value was observed relative to using the global variogram to krige each population separately. These results suggest that it is of primary importance for this particular dataset to identify and krige subpopulations within the data field separately. Further but modest improvements can be made by incorporating the subpopulation variograms instead of the global variogram.

The present study extends the work of Desbarats (1987) who used indicator kriging to develop a two-dimensional, binary model of permeability in sandstone formations containing interbedded shale. He focused on the spatial dependence of shale as the primary control on low permeability in the system. He developed indicator variograms for shale based on both experimental and theoretical data. The resulting permeability was a function of the inferred shale volume fraction. Desbarats primarily uses the geostatistical approach for parameter estimation. He indicates that the shale should be treated separately from the sandstone but does not calculate sandstone variograms or global variograms for comparison.

Analyses conducted for this study suggest that the primary source of error is due to kriging with the complete set of water content measurements rather than kriging with soil-specific values; incorporating soil-specific variograms was only of secondary importance to the final result. Consequently, the third method is the most efficient and forms the basis for kriging selected time planes.

A three-dimensional view of kriged water content is shown in Figure 9 for preinjection conditions (tp1). The kriging was done to a 16 x 16 x 36 regular grid of cells that measures 90 x 90 x 50 cm. This grid is the same as that developed for the three-dimensional model.

The neutron probe count was converted to water content after estimation with kriging. The kriging estimation at the grid nodes indicates a maximum water content of 14% near the surface and, generally, on the order of 5% to 6% at depth. The wet surface is consistent with infiltration into the upper few meters produced by the wet conditions in 1980. The dry soil at depth also is consistent with the deep-rooted plants living at the site prior to construction of the well network.

3.3.3 Spline Estimation of Water Content

These water content data also were estimated in three-dimensions using the earthVision visualization software developed by Dynamic Graphics, Inc. (1993); the software interpolates scattered data using biharmonic cubic splines based on an algorithm developed for machine contouring of geologic data using minimum curvature (Briggs 1974). Schumaker (1981) described the basic theory of splines, including their computational efficiency as well as their utility for data analysis. Matheron (1981) proved the mathematical equivalence of kriging and spline functions, and Cressie (1991, p. 180-183) provided a good discussion of the similarities of the two methods.

Dynamic Graphics, Inc. (1993) incorporates the biharmonic cubic spline into their minimum-tension gridding routine for interpolation. The algorithm calculates an initial estimate for a node based on search of surrounding points using a modified inverse-distance weighting function that factors in the angular distribution of points. Then the initial estimate is refined using a biharmonic cubic spline function. The algorithm minimizes the second derivative (curvature) of this function at the nodes using a sum-of-squares approach.

Three-dimensional views of water content data are shown in Figure 10 for preinjection conditions (tp1) and in Figure 11 for conditions after three injections (tp4). These images are spline-interpolated from neutron probe measurements in all 32 monitoring wells (1920 total data points) at each measurement time. Water content was calculated for each node based on the interpolated neutron probe count. The injection well is located one quarter of the distance from the surface to the bottom.

Kriging and the cubic spline method produced very similar results. Evaluation of the two estimation techniques was conducted by comparing the estimated values for each node in the grid. The comparison was made by subtracting water content values for corresponding cells in the grid. Results of error analyses for tp1, tp2, tp4, and tp8 are listed in Tables 5-8. Results are tabulated for the entire system and selected subdivisions within the system, including each geologic unit and the set of measured points.

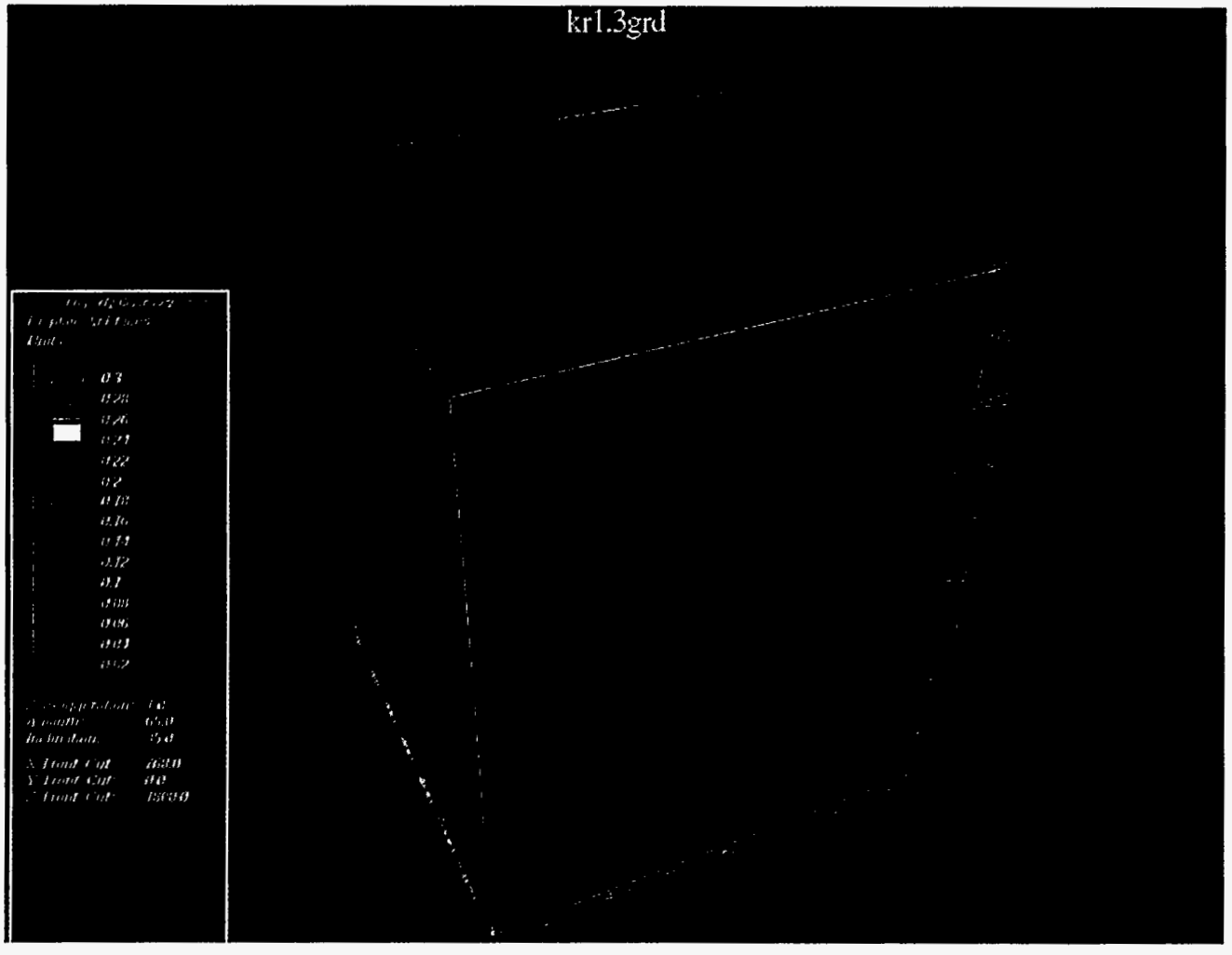

Figure 9. Three-dimensional view of kriged water content, tp1

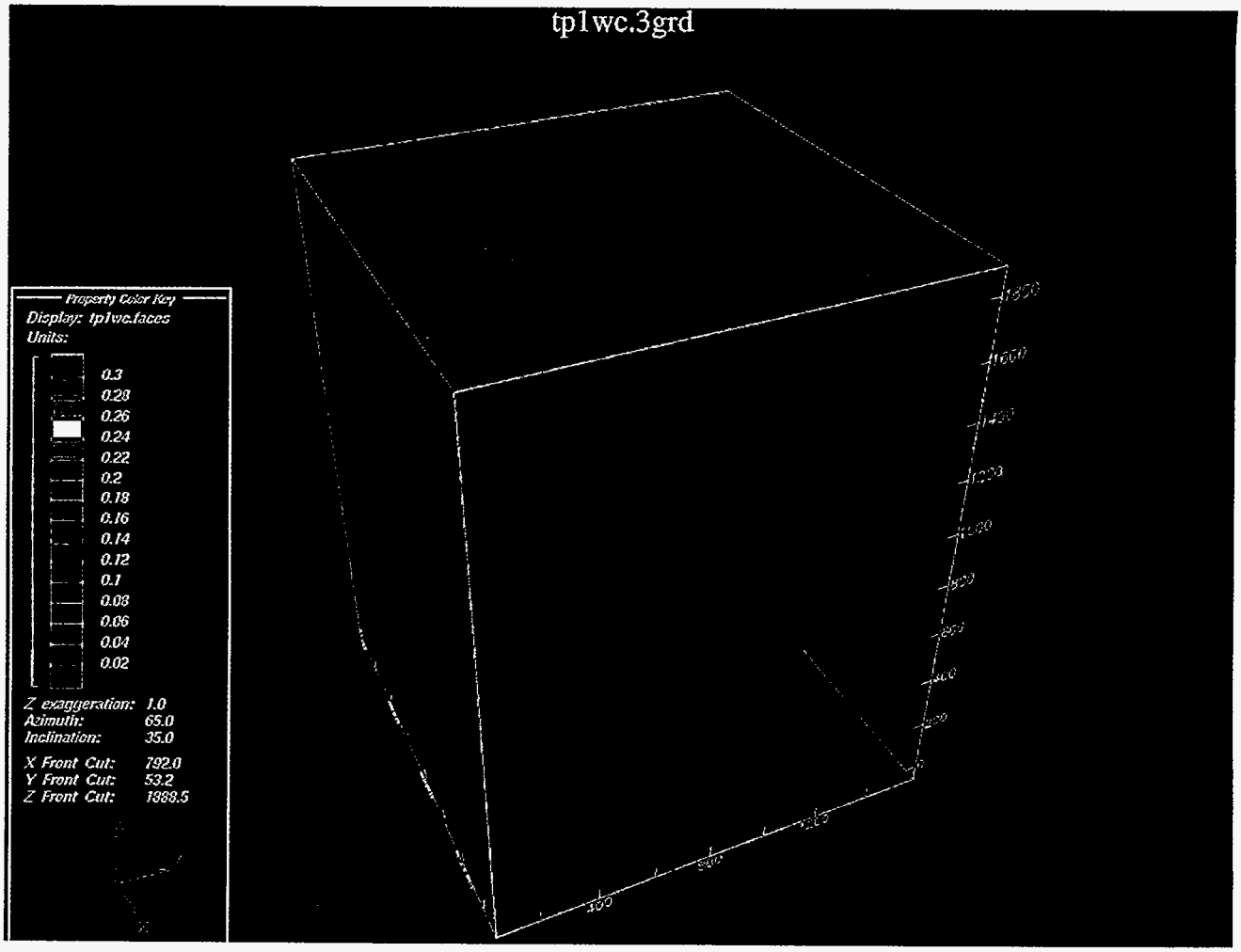

Figure 10. Three-dimensional view of spline-interpolated water content, tp1

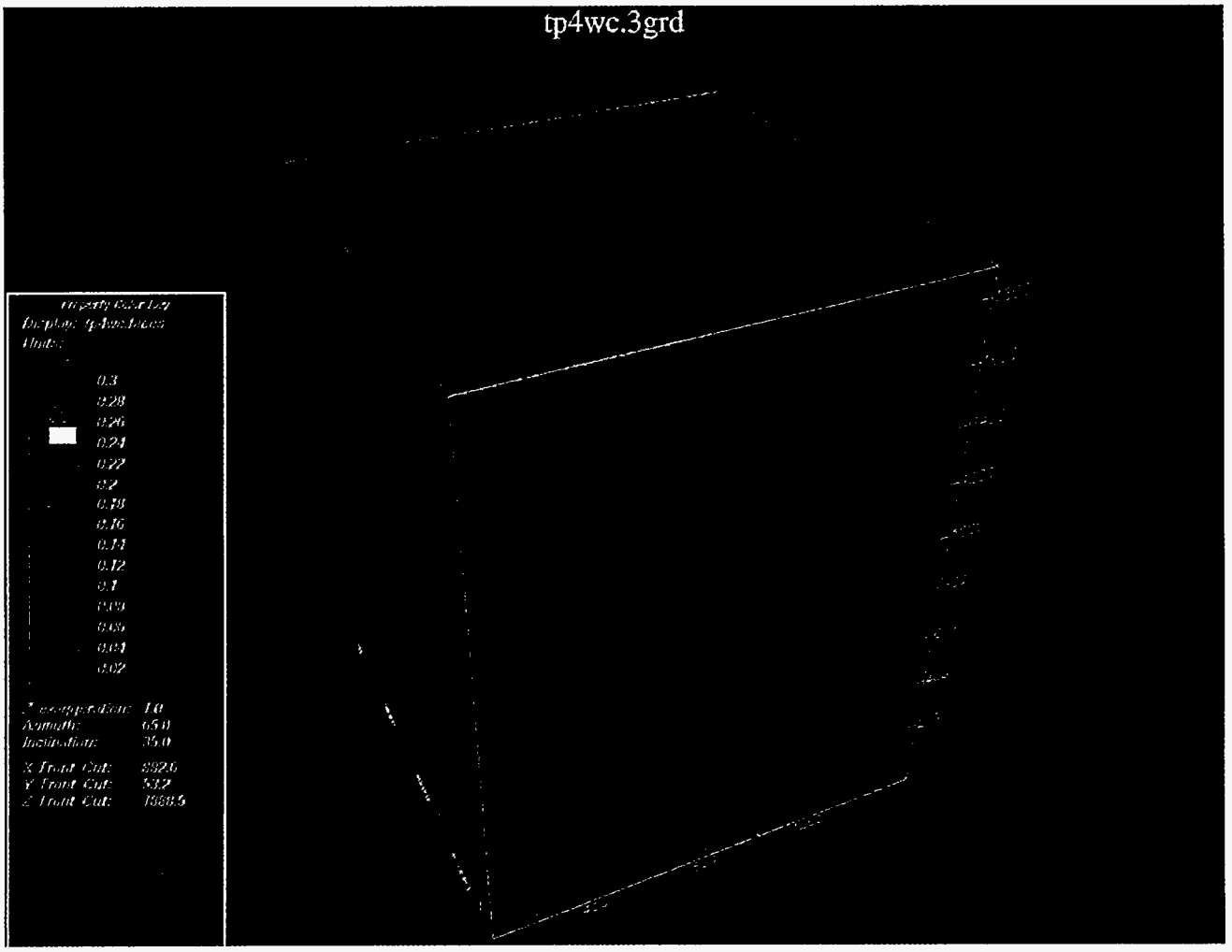

Figure 11. Three-dimensional view of spline-interpolated water content, tp4

Table 5. Error for spline-interpolated minus kriged values, tp1

Subset	# Cells	Sum	Sum Squares	Avg. Err.
All Cells	9216	24.82	2.91	0.00
Measured WC	1152	-0.03	0.22	0.00
West Half	4608	17.48	1.60	0.00
East Half	4608	7.33	1.31	0.00
Bottom Half	4608	5.63	0.54	0.00
Top Half	4608	19.19	2.38	0.00
SW Quadrant	2304	-0.62	0.81	0.00
NW Quadrant	2304	18.10	0.80	0.01
SE Quadrant	2304	1.06	0.61	0.00
NE Quadrant	2304	6.27	0.70	0.00
1: silt	41	-0.05	0.00	0.00
2: sfms	1318	-2.87	1.09	0.00
3: ssms	287	10.39	0.72	0.04
4: mscs	4220	2.64	0.53	0.00
5: msgr	124	-0.18	0.02	0.00
6: csgr	2178	4.46	0.25	0.00
7: mcgi	1048	10.43	0.30	0.01

Table 6. Error for spline-interpolated minus kriged values, tp2

Subset	# Cells	Sum	Sum Squares	Avg. Err
All Cells	9216	22.62	3.22	0.00
West Half	4608	6.96	1.65	0.00
East Half	4608	15.66	1.57	0.00
Bottom Half	4608	5.02	0.49	0.00
Top Half	4608	17.60	2.73	0.00
SW Quadrant	2304	-1.17	0.90	0.00
NW Quadrant	2304	8.13	0.75	0.00
SE Quadrant	2304	9.75	0.87	0.00
NE Quadrant	2304	5.91	0.70	0.00
1: silt	41	-1.17	1.06	0.00
3: ssms	287	7.66	0.61	0.03
4: mscs	4220	4.87	0.79	0.00
5: msgr	124	1.14	0.02	0.01
6: csgr	2178	1.23	0.45	0.00
7: mcgi	1048	9.08	0.28	0.01
Measured WC	1152	0.92	0.54	0.00

silt = silt
sfms = silty, fine-to-medium sand
ssms = silty sand to medium sand
mscs = medium sand to coarse sand
msgr = medium sand to gravel

Table 7. Error for spline-interpolated minus kriged values, tp4

Subset	# Cells	Sum	Sum Squares	Avg. Err.
All Cells	9216	39.06	3.85	0.00
West Half	4608	8.48	1.83	0.00
East Half	4608	30.58	2.02	0.01
Bottom Half	4608	8.25	0.96	0.00
Top Half	4608	30.81	2.89	0.01
SW Quadrant	2304	1.07	0.88	0.00
NW Quadrant	2304	7.40	0.95	0.00
SE Quadrant	2304	16.00	0.92	0.01
NE Quadrant	2304	14.58	1.10	0.01
1: silt	41	-0.67	0.02	-0.02
2: sfms	1318	-1.95	1.16	0.00
3: ssms	287	7.09	0.55	0.02
4: mscs	4220	22.44	1.59	0.01
5: msgr	124	1.07	0.02	0.01
6: csgr	2178	2.33	0.23	0.00
7: mcgi	1048	8.75	0.28	0.01
Measured WC	1152	5.71	0.81	0.00

Table 8. Error for spline-interpolated minus kriged values, tp8

Subset	# Cells	Sum	Sum Squares	Avg. Err.
All Cells	9216	0.95	3.89	0.00
West Half	4608	-19.07	2.05	0.00
East Half	4608	20.03	1.84	0.00
Bottom Half	4608	-10.12	1.21	0.00
Top Half	4608	11.08	2.68	0.00
SW Quadrant	2304	-11.47	0.98	0.00
SE Quadrant	2304	14.09	0.79	0.01
NE Quadrant	2304	5.94	1.05	0.00
1: silt	41	-0.50	0.03	-0.01
2: sfms	1318	-3.47	1.36	0.00
3: ssms	287	6.72	0.67	0.02
4: mscs	4220	-13.41	1.20	0.00
5: msgr	124	0.68	0.01	0.01
6: csgr	2178	1.52	0.34	0.00
7: mcgi	1048	9.41	0.29	0.01
Measured WC	1152	-0.78	0.63	0.00

csgr = coarse sand to gravel
mcgi = interbedded medium sand, coarse sand, and gravel
WC = water content

3.4 Mathematical Model

White et al. (1992) incorporated the partial differential equations that describe unsaturated zone flow and transport into the design and operation of the Subsurface Transport Over Multiple Phases (STOMP) code used in this study to model flow at the injection test site. The code was chosen because it incorporates an integral finite difference formulation that eliminates mass balance error as well as a modular format that allows the optimization of execution speed and memory. These criteria are important for three-dimensional analysis of water contents in the unsaturated zone. The code offers the choice of either a banded matrix solver or a conjugate gradient solver. The banded solver was used for this study. The code was designed to simulate phenomena at both the laboratory and field scale, and ultimately investigate remediation strategies at the field scale.

The mathematical implementation of the hydrogeologic conceptual model utilizes the discretization of the subsurface geology at the injection test site (Section 3.2) along with laboratory measurements of the hydraulic properties of drilling samples. The major components of the model include the lithologic framework, the boundary conditions, the initial conditions, and the injection of the fluid as described below.

Water retention characteristics were measured in the laboratory for selected soil samples collected during drilling of the observation wells at the test site. The hanging water content method, the pressure plate method, and the vapor adsorption method were used to measure the low, intermediate, and high tension conditions, respectively. These laboratory measurements are reported in Fayer et al. (1993). For this study, data from selected samples that describe each soil type were fitted to a water retention function developed by van Genuchten (1980); the function parameters become the input to the mathematical model. The RETC code (van Genuchten, Leij, and Yates 1991) was used to fit the function to these data using Mualem's restriction (m=1-1/n) recommended for structured and coarse-textured soils (Table 9).

Boundary conditions for the model were set for all six faces of the rectangular prism that constitute the domain. These boundary conditions are summarized in Figure 12. No-flow boundaries were established on all vertical boundaries. The lower boundary consists of a unit gradient to allow for free vertical drainage of water (injectate plus infiltration) through the bottom of the model toward the water table. The upper boundary represents net infiltration calculated as a function of precipitation and evapotranspiration. The top boundary of the model consists of a constant flux surface that was set equal to a fraction of the annual precipitation. A value of 5 cm was used based on lysimeter studies that indicate an infiltration range of 4 to 11 cm/yr for bare sand surfaces (Gee 1987) and simulation studies that indicate both vegetation and grain size control infiltration (Smoot et al. 1989).

Equilibrium initial conditions of pressure head and water content were calculated with the code to simulate the initial condition in the sediments prior to the first fluid injection. An initial estimate of 6% water content was applied to all of the sediments. Different solutions were calculated for average annual surface infiltration fluxes of 4.0 and 5.0 cm/yr. Then the model was run to steady-state conditions. This steady

Table 9. Summary of soil hydraulic properties

Soil	Grain Density	Porosity Porosity	K (cm/s)	Alpha (cm-1)	n	Res. Sat.
silt	2650.0	0.37	1.39E-04	0.014	1.55	0.19
sfms	2650.0	0.28	3.23E-04	0.007	2.80	0.21
ssms	2650.0	0.31	3.23E-04	0.007	2.80	0.13
mscs	2650.0	0.26	6.05E-03	0.041	1.94	0.13
msgr	2650.0	0.32	1.31E-02	0.089	1.48	0.08
csgr	2650.0	0.33	2.18E-02	0.024	1.65	0.10
mcgi	2650.0	0.29	6.54E-02	0.126	1.55	0.12

Aqueous Relative Permeability: Mualem's Method
Saturation Function: van Genuchten

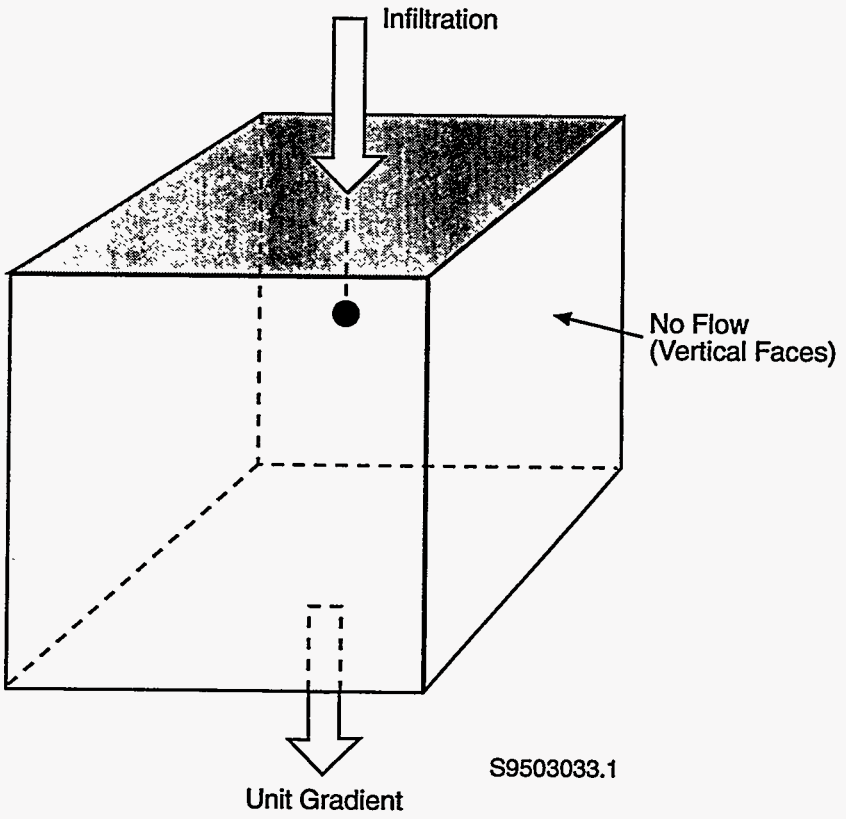

Figure 12. Summary of model boundary conditions

state solution forms the initial condition for the transient simulation. Steady-state solutions were compared to the preinjection water content measurements at the injection test site, as will be discussed in Section 4 of this report.

In the experiment, the fluid was injected as a point source through a hole in the steel plate welded to the base of the casing at the 4.6-m depth. The fluid was injected once every 7 days for 10 weeks for the period September 22 through October 24, 1980. One additional injection was conducted February 2, 1981. Approximately 4000 L were injected each time; the average flux rate was 7000 L/day (Figures 10 and 11). The total flux rate duration and time generally was input to the model as recorded during the experiment. However, some combinations of hydraulic parameters were sensitive to the injection rate, requiring gradual changes at the initiation and conclusion of each pumping stress. The gradational change at the beginning and end of each injection phase was necessary to reduce the shock to the system, and to allow for smooth and timely transition between stress periods so as to reduce computer run times.

Water content was simulated under steady-state conditions to mimic the initial state of the injection test site prior to the first injection. A view showing the distribution of volumetric water content for these calculated initial conditions is shown in Figure 13. Approximately half of the domain has been cut away to reveal a vertical cross section. The cross section is oriented in the east-west direction. These results generally indicate high water content in the fine-grained layers and lower water content in the coarse-grained units, similar to measured data that represent the same time period. The highest water contents are observed in the silt lenses located near the middle of the section.

These results qualitatively are similar to both the kriged and cubic-spline images presented in Figures 9 and 10. Comparison of these figures suggests that the model reasonably mimics the observed conditions. However, the modeled water content in excess of 0.2 in the center of the lenses is higher than measured; the water content in the coarse-grained units is higher, suggesting that the infiltration rate of 5 cm/yr is somewhat too high.

A three-dimensional view of water content for case 4 at tp6 (41.5 days) is shown in Figure 14. Zones of high water content are clearly visible surrounding the injection point, located 500 cm below the surface. Again, the highest water contents are associated with the fine-grained layers and they suggest wetter conditions than observed in the field.

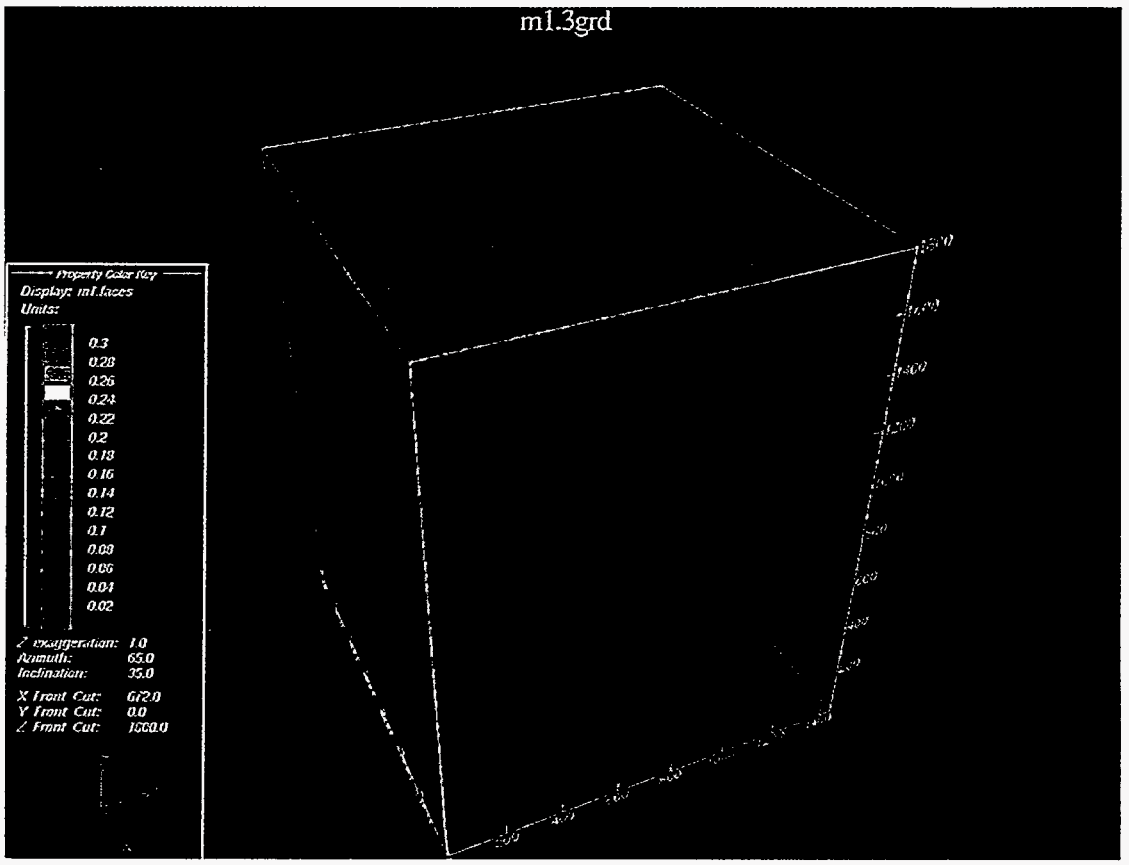

Figure 13. Model simulated water content, tp1

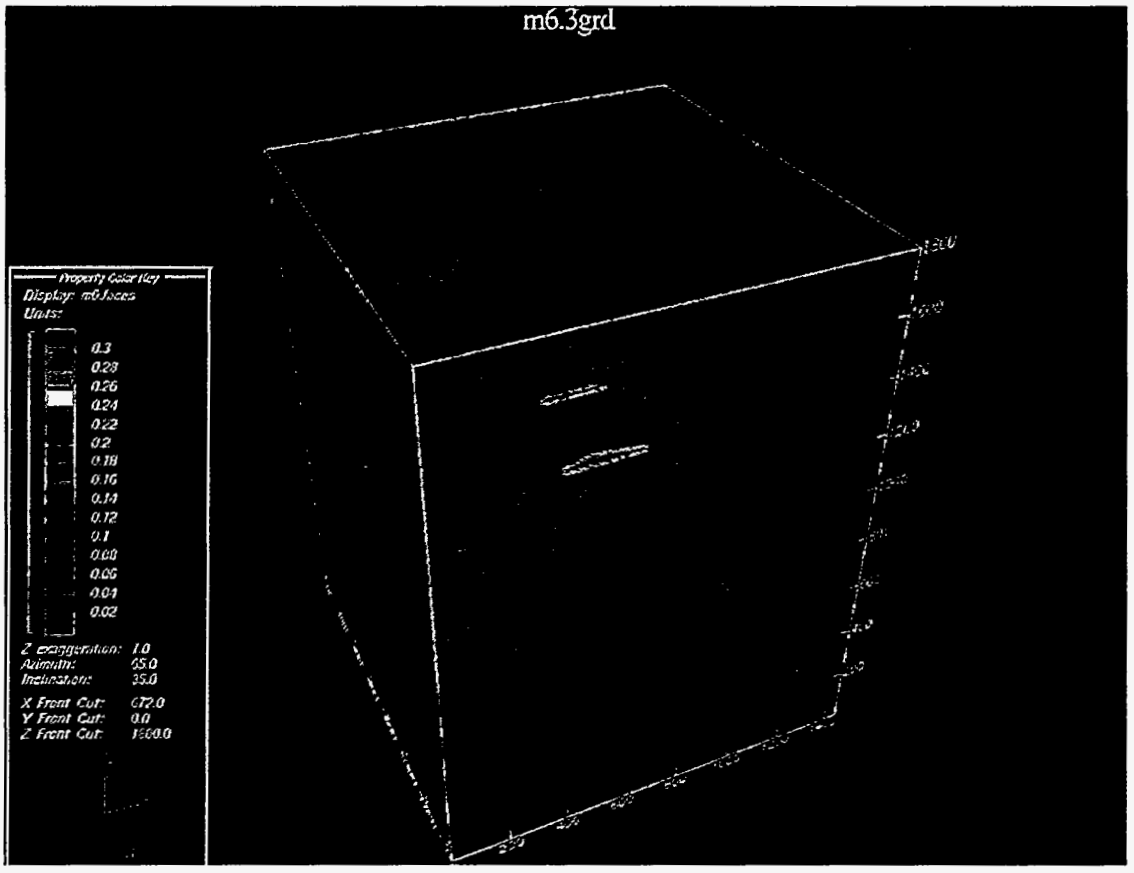

Figure 14. Model simulated water content, tp6

4.0 Evaluation Of Model Results

4.1 Introduction

The purpose of this study is to develop a geostatistical database that allows the researcher to evaluate the accuracy of model output and integrate the results into an understanding of the system. Quantitative knowledge of the relationship between the model and the data is an important component of this understanding. The presentation of model results commonly is very qualitative. For example, one often is subjected to a curve drawn through a cloud of points and the match summarily is described as either good or bad. Obviously, a more quantitative means of understanding the results is needed, especially for large, three-dimensional models. The method described in this section incorporates the geostatistical database developed in the previous section. The geostatistical database and mathematical model share a common grid such that there is a one-to-one correspondence between them in terms of cartesian spatial coordinates and volume. Therefore, every node in the model can be checked against these data or against an estimate and the differences can then be analyzed.

Node-by-node error analysis is used in this study to understand how the model results compare with the geostatistical database. Detailed evaluations of model results usually are not undertaken in modeling studies because data collection commonly is not planned to fulfill both model parameterization needs and model calibration needs. Delhomme (1979) discussed kriging of hydraulic head to assist parameter estimation during model calibration. Node-by-node analysis of differences has been applied to two-dimensional inverse model calibration based on theoretical (Neuman and Yakowitz 1979) and mapped distributions (Neuman et al. 1980) of gridded transmissivity. The error analysis described in this section extends the work of these studies by incorporating the three-dimensional geostatistical database with model validation concepts proposed by Steinhorst (1979) for comparisons between measured data points and corresponding model points.

4.2 Method of Error Analysis

Steinhorst (1979) reviewed the concept of differences both for time series and spatial analyses as they relate to modeling. The first step in the model evaluation process is to calculate a matrix of differences (Y) in the form of equation 7 (Steinhorst 1979), where D refers to the data matrix and M to the matrix of model results.

$$Y = D - M \qquad (7)$$

Calculation of differences in this manner assumes registration between the data and model such that there is one-to-one correspondence between both the coordinates and the volume represented by each number. As a practical matter, once the dimensions and nodal spacing within each grid are fixed, the accounting is accomplished by reference to the equivalent nodal index in each matrix.

The error is analyzed by comparing water content throughout the space of the model at given times and by summarizing average water content error over time. The three-dimensional model was calculated to steady-state conditions in order to mimic the initial state of the system prior to injection of the fluids. The model then was run in a transient mode with stress periods corresponding to the injection periods recorded during the experiment. Model output times were selected to coincide with the times when data were collected.

4.3 Analysis of Differences

The goal of generating differences is to provide a better method of accounting for the accuracy of model results. The analysis of injection test modeling results is described in this section in terms of differences. The numerical model represents the best embodiment of the

hydrogeologic conceptual model. A range of reasonable initial conditions was investigated, as described in Section 6.1.2. The error analysis then facilitates systematic analysis of the different model parameters and clearly identifies the mathematical model result that best represents the hydrogeologic conceptual model. However, the difference matrix must be processed and analyzed to generate this understanding. Error for the whole model first is analyzed as a frame of reference for further study. Statistical analysis and spatial grouping are very important for understanding the model because a large matrix of differences is difficult to understand on its own. This process is similar to trying to analyze the output from a large model by looking at columns of numbers.

Differences were analyzed in several ways. Measured data points first were checked against model predictions at corresponding registered model nodes. Then all model nodes were checked against data interpolated to the same grid using both kriging and cubic splines. Statistics were calculated for all 9216 nodes as a base reference. Then statistics were tabulated for subgroups or bins of model nodes: top half and bottom half, east half and west half, map-view quadrants, and by the stratigraphy that was assigned to each cell based on the hydrogeologic conceptual model. In addition, differences were calculated for nodes in the model corresponding to measured data points in the observation wells.

A number of statistics were calculated to describe the cumulative error in each bin of differences calculated in equation 1: a simple sum of error, a sum of squares of the error, and an average error. The average error is especially useful for cases where the number of cells in each bin is unequal, such as for comparison of results by stratigraphy.

The steady-state model results are summarized in Table 10. The infiltration rate is 5 cm/yr. The average error for the simulation is -0.03 when comparing with the geostatistical database. Comparison solely with measured data points produced the same error as the average error. Tabulation of the error by model halves and quadrants did not discriminate much information about the nature of the errors; these errors were within 0.01 of the average water content. However, these numbers indicate that error is distributed evenly throughout the model and indicate that the large errors observed in the top half of the model in cases 1 and 2 have been significantly reduced.

More significant geologically is the ability to examine errors for each lithologic unit included in the tables. The largest average errors are -0.14 for silt, -0.06 for coarse sand to gravel (csgr), and -0.05 for medium sand to gravel (msgr). Note that silt constitutes only 41 (0.4%) of the nodes, while csgr constitutes 2178 (24%) of the nodes. Average error for silty to medium sand (ssms) and medium to coarse sand (mscs) are both -0.01 and together account for 4507 (49%) of the model cells. Average error for the silty, fine to medium sand (sfms) was -0.03.

Based on these results, a transient analysis was conducted. Results of these analyses are

Table 10. Summary of case 4 steady-state model results

Subset	# Cells	Sum	Sum Squares	Avg. Err.
All Cells	9216	-233.53	13.94	-0.03
Measured WC	1152	-32.56	1.94	-0.03
West Half	4608	-122.11	7.40	-0.03
East Half	4608	-111.42	6.53	-0.02
Bottom Half	4608	-149.68	8.52	-0.03
Top Half	4608	-83.85	5.41	-0.02
SW Quadrant	304	-67.26	3.93	-0.03
NW Quadrant	2304	-54.85	3.47	-0.02
SE Quadrant	2304	-58.85	3.36	-0.03
NE Quadrant	2304	-52.56	3.17	-0.02
1: silt	41	-5.86	0.85	-0.14
2: sfms	1318	-43.26	2.85	-0.03
3: ssms	87	-2.48	0.82	-0.01
4: mscs	4220	-28.85	0.82	-0.01
5: msgr	124	-5.61	0.26	-0.05
6: csgr	178	-124.27	7.46	-0.06
7: mcgi	1048	-23.20	0.88	-0.02

shown in Figures 15 through 18, summarizing the tabulated comparisons for time planes tp1 through tp8.

Comparison of the global average error versus that only at measured points is shown in Figure 14. These errors plot on top of each other, consistent with the fact that they contain the same amount of data. In addition, the errors are invariant over time, indicative of a robust analysis from both a data and modeling standpoint. The datasets for each time plane contain the same amount of data and should be expected to produce similar metrics of model performance at each time step. Consequently, the model appears to reflect the changes in water content in the sediment resulting from the fluid injections. The major systematic error appears to be in the establishment of the initial conditions of the experiment.

Error by map view quadrants over time is shown in Figure 15 plotted together with the global average. The quadrant averages are all less than or equal to the global average, and range from -0.02 to -0.03. Model error by half domains is plotted over time in Figure 16. This breakdown shows some minor transient changes in the error over time. Errors for the top half and the east half were reduced by 0.01 after approximately 50 days, while error for the bottom half increased by 0.01 after approximately 25 days. However, it should be stressed that these errors are relatively small.

Errors over time are grouped by lithology in Figure 17. Again, errors tended to be relatively invariant over time, with slight changes of ± 0.01. The global average error for all cells is included. The worst error is observed for silt, generally about -0.15 over time. Csgr remains constant over time at -0.06. Msgr begins at -0.05, reduces to -0.04 and remains constant to approximately 40 days. Then the error increases to -0.05 at approximately 50 days and further increases to -0.07 beyond 100 days. The errors for the remaining units are generally constant and equal to the value determined in the steady state analysis.

The model error may also be shown visually for each model cell (Figure 19). This figure shows the color-coded value of the difference for each model cell at time plane tp1. The front section of the model domain has been cut away. The areas of dark green and light blue indicate areas where the model error is small while dark blue and purples indicate cells where the modeled water content is too wet and areas of light green, yellow, and orange indicate areas where the modeled water content is too high. This plot suggests that the modeled water content is reasonable for a large percentage of the cells in the model. However, it also reveals several zones where modeled water content is too high and several zones where the modeled water content is too low. There are several reasons for the modeled behavior in these zones.

Comparison of model results with the geostatistical database indicates that the worst model approximations are for fine-grained sediments. One possible reason for this discrepancy is that significant structure exists in these fine-grained layers that is destroyed during drilling; less structure occurs in the coarse-grained sediments. Deposition of coarser material would be expected to occur under high-energy conditions that might produce a more random arrangement of the coarse sand and gravel grains; whereas, layering and other structure could develop in the fine-grained material deposited under low-energy conditions.

Additional reasons are that the fine-grained lenses and layers may not be located accurately or they are too thick given the limitations of the grid. Generally, the model results for these layers show more water retention than suggested by the data. While these data and the model are on the same grid, scaling problems could occur, given that much of the water content change is observed across a 0.3-m increment. However, the fine-grained units also may be misinterpreted spatially in the model. Generally, these units are one layer of nodes thick and factors such as overlap between layers could cause them to be located a layer too high or a layer too low.

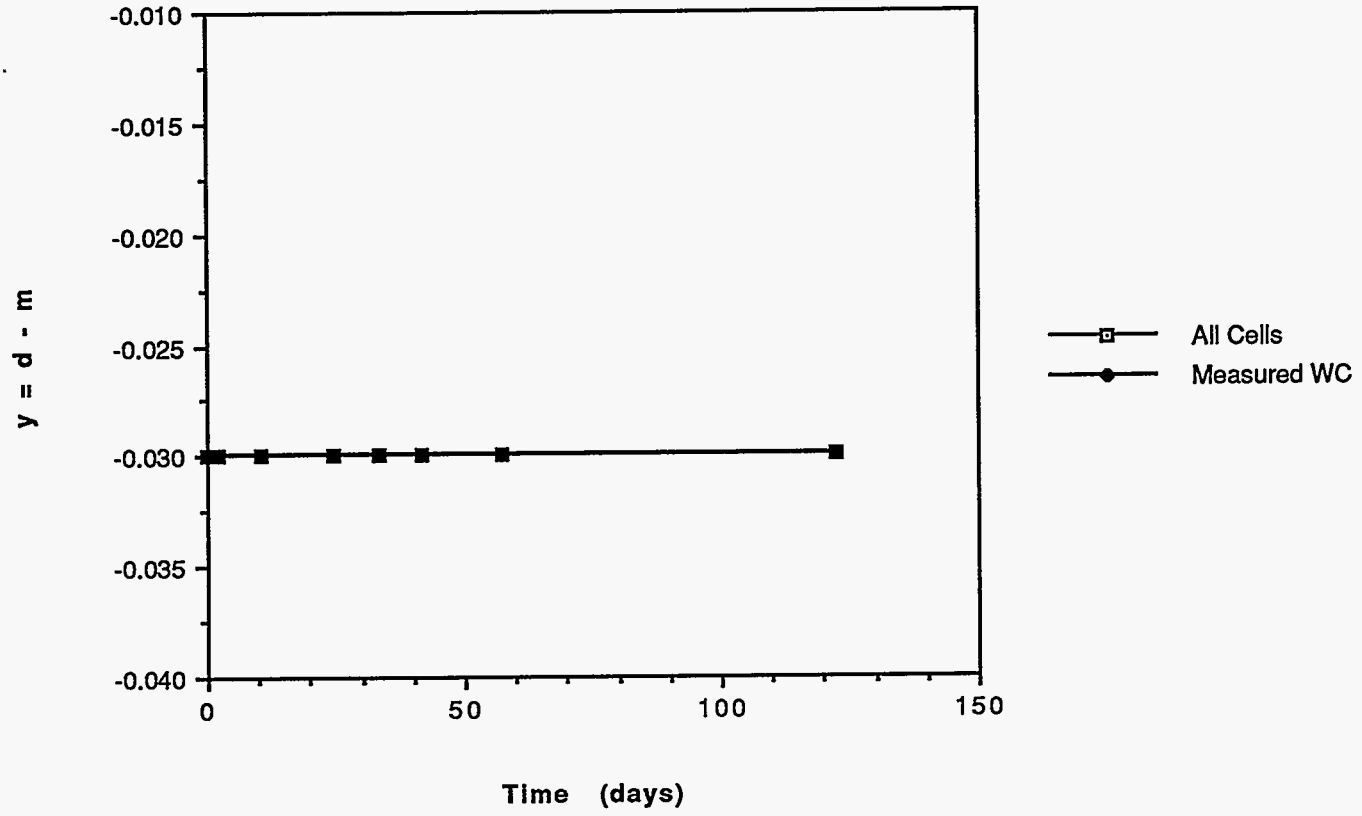

Figure 15. Average error of simulated water contents, tp1-tp8

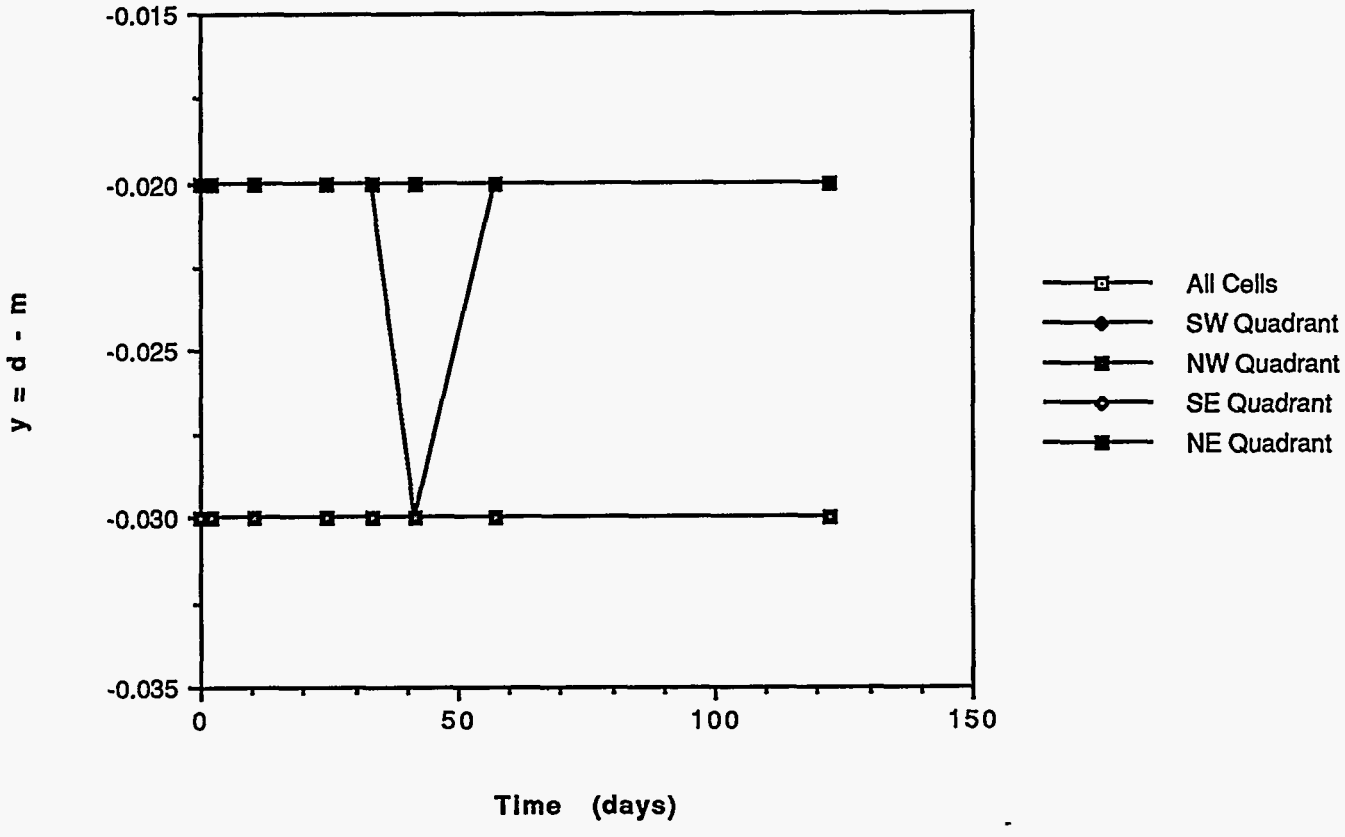

Figure 16. Average error of simulated water contents for map-view quadrants, tp1-tp8

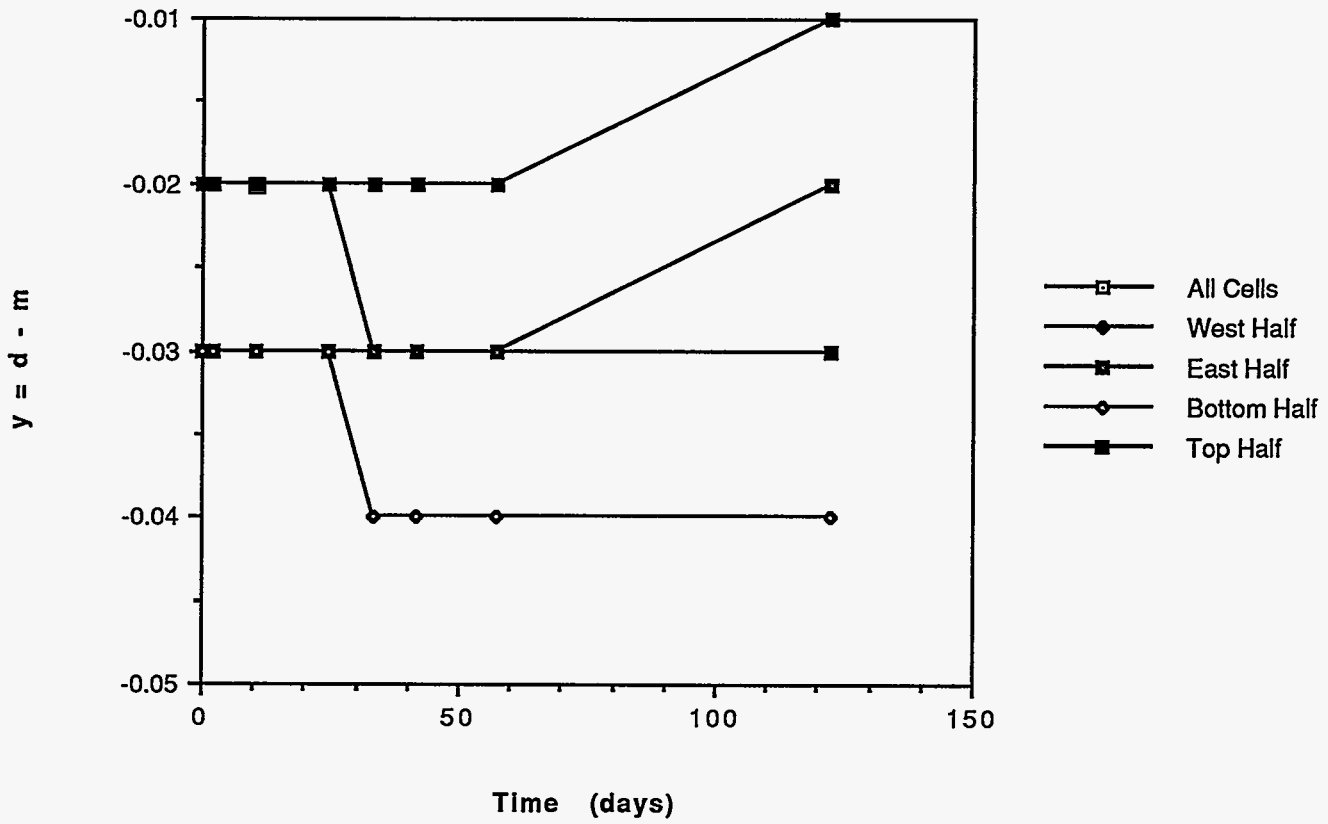

Figure 17. Average error of simulated water contents grouped by half domains, tp1-tp8

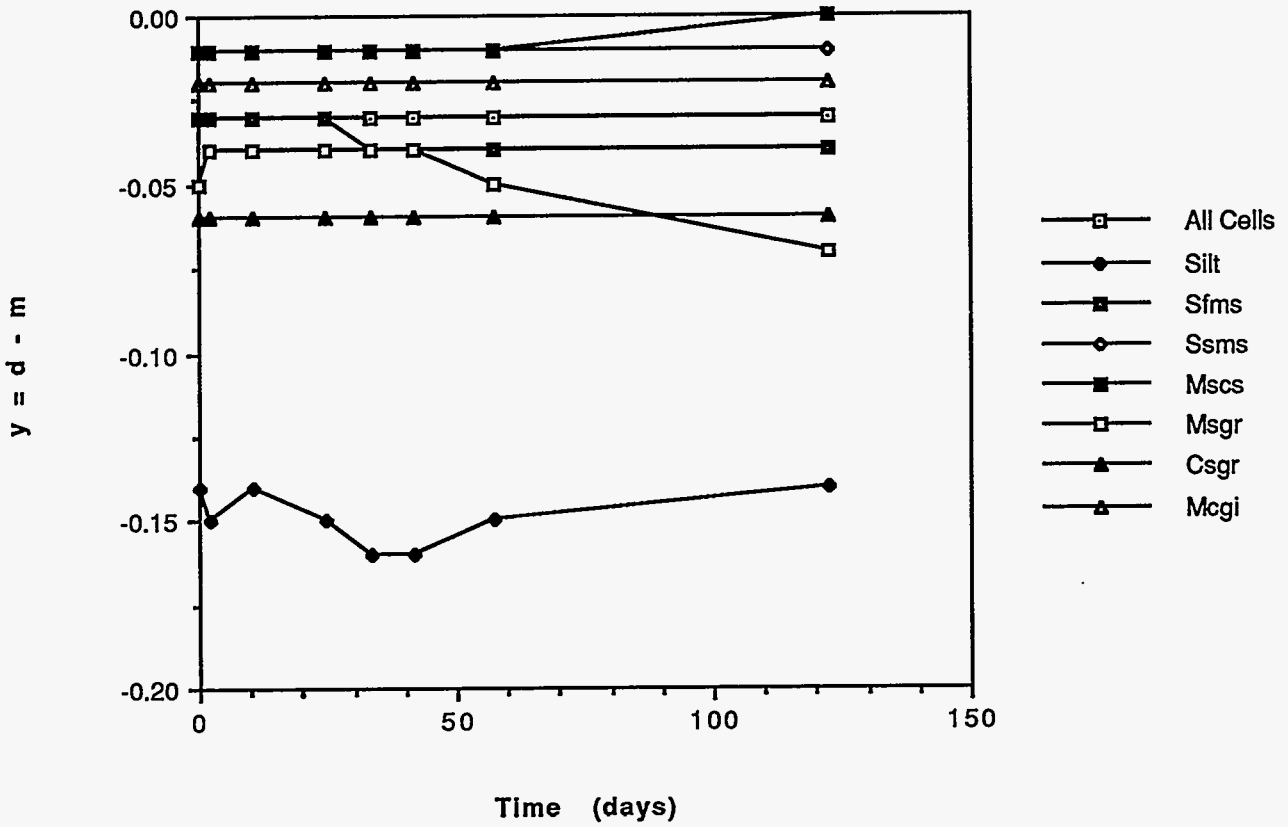

Figure 18. Average error for simulated water contents grouped by lithology, tp1-tp8

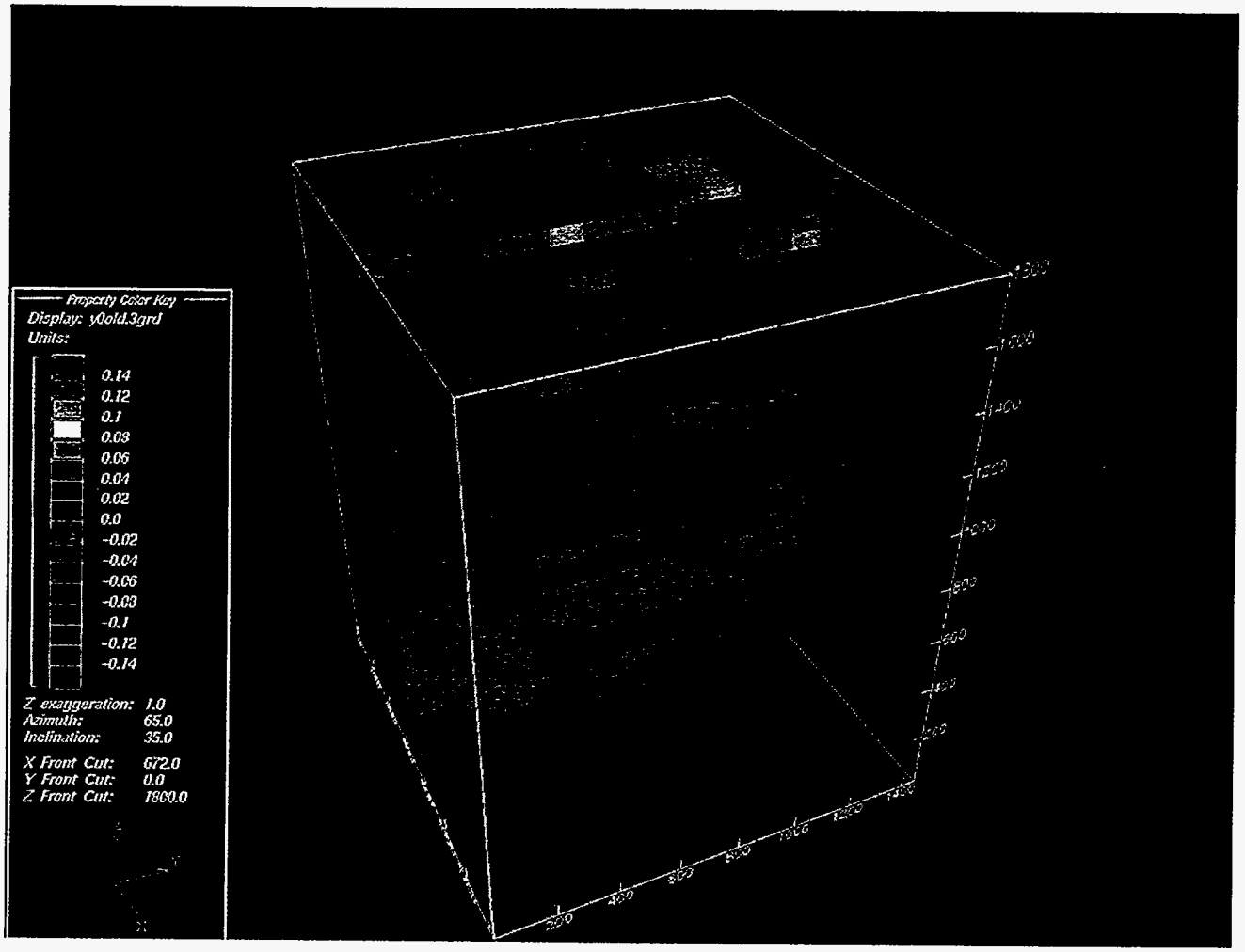

Figure 19. Three-dimensional color plot of model error, tp1

4.4 Significance of Results

Evaluation of mathematical model predictions and the uncertainty of these predictions was investigated in this study. Development of the geostatistical database approach used in this study requires a robust database and integration of a geostatistical analysis with a mathematical modeling analysis. As noted by Wang and Williams (1984), a mathematical modeling analysis supported by a strong field database can be a powerful tool for the knowledgeable regulator. Conversely, a mathematical modeling analysis that is not supported by a strong field database may be easily discredited and subsequently disregarded during the regulatory process. This section first discusses the regulatory impacts from this study. Impacts to this study from data collection procedures at the unsaturated zone test site and general data collection issues for this type of investigation are discussed. The concept of parallel development of mathematical models and geostatistical databases is discussed with regard to this study as well as subsequent studies. Finally, the advantages of the geostatistical database approach are described.

The regulatory significance of this research is the ability of the geostatistical approach to provide a quantitative analysis of the model results for the knowledgeable regulator. The regulations for LLW disposal are codified in 10 CFR 61. These regulations stipulate that "...the disposal site shall be capable of being characterized, modeled, analyzed, and monitored (10 CFR 61.5)." However, the modeling must be conducted in a very thorough manner, substantiated by a relevant field database.

An important problem facing the knowledgeable regulator is that both proponents and opponents of a proposed LLW site will be armed with models supporting their viewpoints. The model of the former will indicate that their site plans comply with all applicable regulatory limits, while the model of the latter will suggest that there are serious shortcomings and that regulatory limits will be exceeded. Bair (1994) recently served as an expert witness at a trial where the jury was presented with results from competing mathematical models. One model was clearly better constructed with proper site-specific data, proper mathematical construction, and better documentation; the jury was able to discern this based on testimony at the trial. Respect for the scientific method and common sense led the jury to a reasonable conclusion about the best validated model.

The drilling logs, geophysical logs, and neutron probe logs collected during the experiment provide the basis for development of the necessary detail in the geologic conceptual model. Prior to this study, these data were not evaluated in an integrated way. Based on their conceptual model, Sisson and Lu (1984) fully expected the site to be homogeneous and isotropic; the site location was chosen because it was expected to exhibit these characteristics. Sisson and Lu did recognize that some layering existed. However, detailed inspection of their data for this study reveals a much more complex stratigraphic sequence. This finding demonstrates that preconceived (or previously published) conceptual models always should be updated as more information becomes available.

The geologic conceptual model developed for the site is based on the hypothesis that the observed stratigraphic units at the test site are a sequence of approximately three or four flood deposits, each characterized as a fining-upward sequence. The fine-grained sediments toward the top of each sequence would be expected to have the highest water retention characteristics because their smaller average pore size would result in higher capillary forces to retain water. The average gamma-gamma response, the three-dimensional porosity field, and the water content distribution suggest that this is a valid hypothesis.

The model results indicate that those nodes defined as silt tend to have the worst absolute error. This could result from both conceptual model error or mathematical model error. The field data suggests that the silt lenses are

relatively thin, measuring 10-20 cm in thickness. However, the smallest increment for thickness in the model is the 50-cm thickness of one cell. Consequently, the greater thickness of fine-grained material in the model would be expected to retain more water than observed in the field, and this effect is observed in the model results. A related source of error is the case where a silt lens straddles the boundary between two nodes. The node assigned to silt would then be either higher or lower than the actual position of the silt in space. This could lead to some inaccuracies in the comparison. However, silt constitutes less than 0.5% of the nodes in the model, so the relative contribution of this error is small.

The lithology defined at each node generally translates well from the conceptual model. Some error could have been reduced by using a finer grid to account for the thin lenses of silt. However, this may have increased the size of the computational grid beyond the present capability of the computer. The 16 x 16 x 36 nodal array pushes the limits of reasonable computational speed. Expected increases in computational capacity over the next few years will allow further research in this area. In addition, better systems are needed to integrate geology into model grids. Currently, the system for assigning lithology to each node is very cumbersome and does not allow for efficient revision of node assignments as the geologic conceptual model evolves. A three-dimensional, interactive graphics system with a mouse could be designed to adjust the orientation and extent of structural contact surfaces. The lithologic assignment at affected nodes would be updated and an indexed file of nodal lithology assignments written to disk for inclusion in a model input file. The lithologic assignment at each node also should be accessible directly for more detailed changes.

The results obtained herein highlight the utility of deterministic models when a sufficient amount of geologic insight is available to formulate the geologic conceptual model. By applying fundamental principles of geology, the database was integrated into a model that successfully simulated a three-dimensional, transient, water-content field within measurement error. Without the geologic insight derived from the site characterization database, the study might have had to rely on stochastic or probabilistic investigations of heterogeneity. This point is important due to the difficulty in persuading knowledgeable regulators and juries to make judgements based on the more theoretical stochastic and probabilistic models. The acceptability of these models in a regulatory framework is still very much in question.

The development of a reasonable geologic conceptual model is dependent on the ability to differentiate and locate lithologic units. Typically, a Bayesian approach is taken by developing an initial concept derived from experience, similarities to known sites, and literature review of regional studies or studies at adjacent sites. Then, the initial inferences are updated as site-specific information becomes available. During this time, it is important to differentiate low and high hydraulic conductivity zones and low and high water retention zones. Several tools can be used to guide this analysis: nearby or analogous outcrops, borehole geophysics, surface geophysics, computer models that simulate sediment deposition, and the geostatistical technique of conditional simulation that could be used to develop a probability density function for lithology type at each node.

Data collection should be consistent with the nodal spacing used in the analysis. The amount of data required and the density of the model grid are dependent on the degree of heterogeneity in the system. The potential for heterogeneity should be anticipated as much as possible to ensure an adequate budget for data collection. This often is an iterative process as the initial estimate of nodal spacing is updated as site characterization data become available.

Analysis of the lithologic subdivisions indicates that the worst model predictions are for fine-grained sediments. One possible reason for this high error is that significant structure exists in these fine-grained layers that is destroyed during drilling; less structure occurs in the

coarse-grained sediments. Deposition of the coarser material would be expected to occur under higher energy conditions that might produce a more random arrangement of the coarse sand and gravel grains whereas layering and other structure could develop in the fine-grained material deposited under lower energy conditions.

An important contribution of this study is value added to model results by making them understandable. Model results are an approximation; the geostatistical database provides the means to evaluate quantitatively the degree of approximation. Consequently, the model results can be explained clearly. Such explanation is very important in describing model results to decision makers. Once the results are understood, considerations of model limitations and uncertainty can be accommodated. Only then should model results contribute to an informed decision.

5.0 Conclusions and Recommendations

5.1 Conclusions

The general conclusion of this study is that node-by-node evaluation of model output using a geostatistical database is a better, more quantitative method to evaluate the accuracy of model output. Many investigators previously have incorporated geostatistics into parameter estimation for input to models of subsurface flow and transport. For sites where data are available, geostatistics can be used to provide an improved basis of evaluation of model output. The method requires a balanced data collection effort geared toward both model input parameterization needs and analysis of model output needs. This balanced data needs approach should be used to guide data collection efforts for modeling studies incorporating a geostatistical database.

Specific conclusions of the study include:

- The site characterization and monitoring data at the Hanford unsaturated zone test site generally are sufficient to identify both the independent variables for model input and the dependent variable for model output (water content). A sufficiently detailed geologic conceptual model was developed to define the lithology at each node. Geophysical investigation provided an effective means of identifying major changes in lithology. The spatial extent of thin silt lenses is difficult to translate effectively to the model geometry, given the limitations on grid size and spacing.

- Data collection for new studies should be guided by the need to define or estimate measured values at all grid nodes.

- The geostatistical database offers a theoretically sound method for comparing measured data to model results on a full grid. The geologic framework and the underlying spatial dependence structure are incorporated into the estimation procedure.

- Utilization of the geostatistical database method requires parallel construction of the mathematical model and the geostatistical database on a common grid.

- The analysis of the spatial dependence structure should be used as an aid in defining the node spacing. Spacing of the nodes in excess of the range of the variogram may reduce the effectiveness of the method because spatially uncorrelated sediment would be associated with a given node.

- Utilization of point or block kriging should be consistent with the use of node or volume formulations for the mathematical model.

- The average error in the model output predictions of water content are within the measurement error of the neutron probe. The worst model error was found to occur in silt lenses.

- Analysis with the geostatistical database constructed for this study suggests that the unsaturated zone mathematical model of the injection test site is reliable for estimating water contents in a heterogeneous environment. The model is based on a robust field database from site characterization, a well-documented conceptual model, and a numerical code that embodies the appropriate theoretical framework.

5.2 Recommendations

Research at the injection test site suggests that the field database is useful for testing models. The results of the research also suggest several areas of research that will be useful for future

studies. Additional research with the existing database should be conducted, including:

- Reconstruction of the three-dimensional geostatistical database with successively depopulated portions of the water content field database to determine whether excessive data was collected at the injection test site.

- Reconstruction of the three-dimensional geostatistical database by cokriging water content with gamma-gamma log analysis.

- Reconstruction of the three-dimensional geostatistical database with conditional simulation studies to investigate whether the reduced smoothing of this method favorably impacts model analysis.

Several recommendations with regard to future studies are as follows:

- Design data collection strategies for combined mathematical modeling and geostatistical analyses, and strongly consider the use of surface geophysics to enhance the level of detail and completeness of coverage.

- Investigate the role of the spatial dependence structure in defining nodal spacing.

- Investigate the sensitivity of comparisons to construction of the geostatistical database with point kriging versus block kriging at different scales.

- Develop interactive methods to assign geologic and hydrologic properties to model nodes.

- Develop weighting functions for values at measured nodes versus estimated nodes within the geostatistical database.

6.0 References

Alexander, D. H., E. R. Hill, J. L. Smoot, D. R. Smith, K. Waldo, B. A. Cerny, and K. M. Krupka. 1991. Three-Dimensional Visualization: Breakthrough in Analysis and Communication of Technical Information for Nuclear Waste Management. In Mat. Res. Soc. Symp. Proc., Vol. 212, p. 797-808.

Bair, E. S. 1994. Model (In)Validation--A View From the Courtroom. GW 32(4):530-531.

Bredehoeft, J. D., and L. F. Konikow. 1993. Ground-Water Models: Validate or Invalidate. GW 31(2):178-179.

Briggs, I. C. 1974. Machine Contouring Using Minimum Curvature. Geophysics 39(1):39-48.

Chu, J, W. Xu, and A. G. Journel. 1994. 3-D Implementation of Geostatistical Analyses--The Amoco Case Study. In Stochastic Modeling and Geostatistics: Principles, Methods, and Case Studies. Edited by J. M. Yarus and R. L. Chambers. Tulsa, Oklahoma: The American Association of Petroleum Geologists, p. 201-216.

Cooper, R. M., and J. D. Istok. 1988. Geostatistics Applied to Groundwater Contamination. I: Methodology. J. Environ. Engrg. 114(2):270-285.

Cressie, N. A. C. 1991. Statistics for Spatial Data. New York: John Wiley & Sons, Inc., 900 p.

Delhomme, J. P. 1978. Kriging in the Hydrosciences. Advan. in Water Resour. 1(5):251-266.

Delhomme, J. P. 1979. Spatial Variability and Uncertainty in Groundwater Flow Parameters: A Geostatistical Approach. Water Resour. Res. 15(2):269-280.

Desbarats, A. J. 1987. Numerical Estimation of Effective Permeability in Sand-Shale Formations. Water Resour. Res. 23(2):273-286.

Desbarats, A. J., and S. Bachu. 1994. Geostatistical Analysis of Aquifer Heterogeneity From the Core Scale to the Basin Scale: A Case Study. Water Resour. Res. 30(3):673-684.

Dynamic Graphics, Inc., 1994, earthVision: User's Guide 2.0, Volume 1, Alameda, CA.

Fayer, M. J., J. B. Sisson, W. A. Jordan, A. H. Lu, and P. R. Heller. 1993. Subsurface Injection of Radioactive Tracers. NUREG/CR-5996, U.S. Nuclear Regulatory Commission, Washington, DC.

Fayer, M. J., R. E. Lewis, R. E. Engleman, A. L. Pearson, C. J. Murray, J. L. Smoot, R. Randall, W. H. Wegener, and A. H. Lu. 1995. Re-Evaluation of a Subsurface Injection Experiment for Testing of Flow and Transport Models. PNL-10860, Pacific Northwest National Laboratory, Richland, Washington.

Gee, G. W. 1987. Recharge at the Hanford Site: Status Report. PNL-6403, Pacific Northwest Laboratory, Richland, Washington.Gee, G. W., M. J. Fayer, M. L. Rockhold, and M. D. Campbell. 1992. Variations in Recharge at the Hanford Site. Northw. Sci. 66(4):237-250.

Gee, G. W., P. J. Wierenga, B. J. Andraski, M. H. Young, M. J. Fayer, and M. L. Rockhold. 1994. Variations in Water Balance and Recharge Potential at Three Western Desert Sites. Soil Sci. Soc. Am. J. 58(1):63-72.

Gilbert, R. O., and J. C. Simpson. 1985. Kriging for Estimating Spatial Pattern of Contaminants: Potential and Problems. Env. Mon. and Assess. 5:113-135.

Isaaks, E. H., and R. M. Srivastava. 1989. Applied Geostatistics. Oxford, U.K.: Oxford University Press, 561 p.

Journel, A. G., and Ch. J. Huijbregts. 1978. Mining Geostatistics. New York: Academic Press, 590 p.

Krige, D. G. 1951. A Statistical Approach to Some Mine Valuation and Allied Problems on the Witwatersrand. M.Sc. Eng., Univ. of the Witwatersrand, Johannesburg.

Larsson, A. 1992. The International Projects INTRACOIN, HYDROCOIN, and INTRAVAL. Adv. in Water Resour. 15:85-87.

Matheron, G. 1963. Principles of Geostatistics. Econ. Geol. 58: 1246-1266.

Matheron, G. 1971. The Theory of Regionalized Variables and Its Applications. ENSMP, Paris. Les Cahiers du CMM, Fasc. No. 5.

Matheron, G. 1981. Splines and Kriging: Their Formal Equivalence. In Down-To-Earth Statistics: Solutions Looking for Geological Problems. Edited by D. F. Merriam. Syracuse: Syracuse University Geology Contributions, p. 77-95.

McCombie, C., and I. McKinley. 1993. Validation-Another Perspective. GW 31(4):530-531.

Mullineaux, D. R., R. E. Wilcox, W. F. Ebaugh, R. Fryxell, and M. Rubin. 1978. Age of the Last Major Scabland Flood of the Columbia Plateau in Eastern Washington. Quarternary Res. 10:171-180.

Murray, C. J. 1994. Identification and 3-D Modeling of Petrophysical Rock Types. In Stochastic Modeling and Geostatistics: Principles, Methods, and Case Studies. Edited by J. M. Yarus and R. L. Chambers. Tulsa, Oklahoma: The American Association of Petroleum Geologists, p. 323-337.

Neuman, S. P. 1980. A Statistical Approach to the Inverse Problem of Aquifer Hydrology: 3. Improved Solution Method and Added Perspective. Water Resour. Res. 16(2):331-346.

Neuman, S. P. 1982. Statistical Characterization of Aquifer Heterogeneities: An Overview. In Recent Trends in Hydrogeology, Special Paper 189. Edited by T. N. Narasimhan. Boulder, Colorado: The Geological Society of America, Inc., p. 81-102.

Neuman, S. P. 1984. Role of Geostatistics in Subsurface Hydrology. In Geostatistics for Natural Resource Characterization. Edited by G. Verly, M. David, A. G. Journel and A. Marechal. NATO ASI Ser., Ser. C, 182, D. Reidel Publishing Company, p. 787-816.

Neuman, S. P., G. E. Fogg, and E. A. Jacobson. 1980. A Statistical Approach to the Inverse Problem of Aquifer Hydrology: 2. Case Study. Water Resour. Res. 16(1):33-58.

Neuman, S. P., and S. Yakowitz. 1979. A Statistical Approach to the Inverse Problem of Aquifer Hydrology: 1. Theory. Water Resour. Res. 15(4):845-860.

Noble, A. C., and D. E. Ranta. 1992. Zoned Kriging-A Successful Union of Geology and Geostatistics. In Applied Mining Geology: General Studies, Problems of Sampling and Grade Control, Ore Reserve Estimation. A compliation of three post-symposia volumes of the Fall Meetings in 1983, 1984, and 1985. Edited by A. J. Erickson Jr., R. A. Metz and D. E. Ranta. Littleton, Colorado: Society for Mining, Metallurgy, and Exploration, Inc., p. 115-128.

Oreskes, N., K. Shrader-Frechette, and K. Belitz. 1994. Verification, Validation, and Confirmation of Numerical Models in the Earth Sciences. Sci. 263:641-646.

Rockhold, M. L., R. E. Rossi, R. G. Hills, and G. W. Gee. 1994. Similar-Media Scaling and Geostatistical Analysis of Soil Hydraulic Properties. Pasco, Washington: Battelle Press, Columbus, Ohio, p. 1099-1129.

Samper, F. J. C., and J. R. Carrera. 1990. Geoestadistica: Aplicaciones a la Hidrogeologia Subterranea. Barcelona, Spain: Centro Internacional de Metodos Numericos en Ingenieria, 484 p.

Scheibe, T. D. 1993. Characterization of the Spatial Structuring of Natural Porous Media and its Impacts on Subsurface Flow and Transport. Ph.D. Dissertation, Stanford University.

Schumaker, L. L. 1981. Spline Functions: Basic Theory. New York: John Wiley & Sons, 553 p.

Sisson, J. B., and A. Lu. 1984. Field Calibration of Computer Models for Application to Buried Liquid Discharges: A Status Report. RHO-ST-46 P, Rockwell Hanford Operations, Richland, Washington.

Smoot, J. L. 1995 Development of a Geostatistical Accuracy Assessment Approach for Modeling Water Conent in Unsaturated Lithologic Units. Ph.D. Dissertation, University of Idaho, Moscow, Idaho.

Smoot, J. L., J.E. Szecody, B. Sagar, G. W. Gee, and C. T. Kincaid. 1989. Simulations of Meteoric Water and Contaminant Plume Movement in the Vadose Zone at Single-Shell Tank 241-T-106 at the Hanford Site. WHC-EP-0332, Westinghouse Hanford Company, Richland, Washington.

Steinhorst, R. K. 1979. Parameter Identifiability, Validation, and Sensitivity Analysis of Large System Models, in Systems Analysis of Ecosystems. Fairland, Maryland: International Co-operative Publishing House, p. 33-58.

Tsang, C.-F. 1991. The Modeling Process and Model Validation. GW 29:825-831.

van Genuchten, M. Th. 1980. A Closed-Form Equation for Predicting the Hydraulic Conductivity of Unsaturated Soils. Soil Sci. Soc. Am. J. 44:892-898.

van Genuchten, M. Th., F. J. Leij, and S. R. Yates. 1991. The RETC Code for Quantifying the Hydraulic Functions of Unsaturated Soils. EPA/600/2-91/065, Robert S. Kerr Environmental Research Laboratory, U.S. Environmental Protection Agency, Ada, Oklahoma.

Waitt, R. B., Jr. 1984. Periodic Jokulhlaups from Pleistocene Glacial Lake Missoula-New Evidence from Varved Sediment in Northern Idaho and Washington. Quarternary Res. 22 : 46-58.

Wang, C.-P., and R. E. Williams. 1984. Aquifer Testing, Mathematical Modeling, and Regulatory Risk. GW 22(3):285-296.

White, M. D., R. J. Lenhard, W. A. Perkins, and K. R. Roberson. 1992. Arid-ID Engineering Simulator Design Document. PNL-8448, Pacific Northwest Laboratory, Richland, Washington.

Zirschky, J. H., Jr. 1985. Geostatistics for Environmental Moniotoring and Survey Design. Env. Intl. 11:515-524.

Distribution

OFFSITE

T. J. Nicholson (5)
U.S. Nuclear Regulatory Commission
Office of Nuclear Regulatory Research
Mail Stop NL-005
Washington, DC 20555

U.S. Nuclear Regulatory Commission
Director, Division of Regulatory Applications
Office of Nuclear Regulatory Research
Mail Stop NL/S-260
Washington, DC 20555

U.S. Nuclear Regulatory Commission
Chief, Waste Management Branch
Division of Regulatory Applications
Office of Nuclear Regulatory Research
Mail Stop NL/S-260
Washington, DC 20555

U.S. Nuclear Regulatory Commission
Director, Division of Low Level Waste
Management and Decommissioning
Office of Nuclear Material Safety & Safeguards
Mail Stop 44-3
Washington, DC 20555

U.S. Nuclear Regulatory Commission
Document Control Center
Division of Low Level Waste Management
Office of Nuclear Material Safety & Safeguards
Mail Stop 44-3
Washington, DC 20555

R. Cady (5)
U.S. Nuclear Regulatory Commission
Office of Nuclear Regulatory Research
Mail Stop NL/S-260
Washington, DC 20555

W. A. Alley
US Geological Survey
Water Resources Division
411 National Center
Reston, VA 22092

J. Andersson
QuantiSci AB
S-125 33 Älvsjö
Sweden

B. Andraski
US Geological Survey
333 W. Nye Lane
Carson City, NV 89706

M.D. Ankeny
Daniel B. Stephens and Associates
6020 Academy NE, Suite 100
Albuquerque, NM 87109

J. Bruno
QuantiSci SL
Parc Tecnológic del Vallés
08290 Cerdanyola
Spain

T. Cameron-Bloomer
U.S. Environmental Protection Agency
6602J
401 M St. SW
Washington, DC 20460

G. S. Campbell
Agronomy Department
Washington State University
Pullman, WA 99164

M. A. Celia
Dept. of Civil Engineering and Operations
Research
Princeton University
Princeton, NJ 08544

N.A. Chapman
QuantiSci Limited
47, Burton Street
Melton Mowbray
Leicestershire LE13 1AP
United Kingdom

D. E. Daniel
Civil Engineering Dept.
University of Texas
Cockrell Hall, Rm. 6-2
Austin, TX 78712

P. Davis
Sandia National Laboratory
Division 6416
P.O. Box 5800
Albuquerque, NM 87185

R. Dettenmeier
Union Electric Company
P.O. Box 149, MC470
St. Louis, MO 63166

M. Dunkelman
Washington State Dept. of Health
Airdustrial Park, Bldg. 5
P.O. Box 47827
Olympia, WA 98504-7827

T. Ellsworth
University of Illinois at Urbana-Champaign
S-210 Turner Hall
1102 S. Goodwin Ave.
Urbana, IL 61801

A.N. Findikakis
Bechtel Corp.
50 Beale St.
P.O. Box 193965
San Francisco, CA 94119-3965

R. A. Freeze
R. Allen Freeze Engineering
3755 NicoWynd Dr.
White Rock, BC
V4P 1J1 Canada 0

R. B. Gilbert
The University of Texas at Austin
Department of Civil Engineering
Cockrell Hall 9.227
Austin TX 78712-1076

E. A. Hausler
Dames & Moore
633 17th Street Suite 2500
Denver, CO 80202-3625

R. G. Hills
Department of Mechanical Engineering
Box 30001, Department 3450
New Mexico State University
Las Cruces, NM 88003

D.P. Hodgkinson
QuantiSci Limited
Chiltern House
15, Station Road
Henley-on-Thames
Oxfordshire RG9 1AT
United Kingdom

P. W. Huntoon
Geology Department
University of Wyoming
Laramie, WY 82071

C. A. Job
U.S. Environmental Protection Agency
Technical and Info. Mgt. Branch
401 M St., SW (4602)
Washington, DC 20460
R. Johnson
Argonne National Laboratory
Environmental Assessment Division
9700 South Cass Avenue
Building 900
Argonne, IL 60439

T. L. Jones
Department of Crop and Soil Sciences
Box 3Q
Las Cruces, NM 88003

W. A. Jury
Department of Soils
University of California
Riverside, CA 92502

D. Keller
Los Alamos National Lab
MS J595
Los Alamos, NM 87545

K. Keller
Geology Department
Washington State University
Pullman, WA 99164

J. Kool
HydroGeoLogic, Inc.
1165 Herndon Parkway
Suite 900
Herndon, VA 22070

J. Korkisch
Institute of Analytical Chemistry
University of Vienna
A-1090 Vienna, Währingerstrasse 38
AUSTRIA

M. W. Kozak and M. J. Apted
QuantiSci, Inc.
3900 S. Wadsworth Blvd., Suite 555
Denver, CO 80235

F. Leij
U.S. Salinity Lab - USDA
4500 Glenwood Drive
Riverside, CA 92501

M. MacDowell
P.O. Box 87
Pittsboro, NC 27312

G. Mahintakumar
Oak Ridge National Laboratory
Center for Computational Sciences
MS 6203
Oak Ridge, TN 37831

R.D. Manteufel
Center for Nuclear Waste Regulatory Analysis
6220 Culebra Rd.
San Antonio, TX 78238-5166

T. J. McCartin
U.S. Nuclear Regulatory Commission
Office of Nuclear Regulatory Research
Mail Stop NL/S-260
Washington, DC 20555

J. T. McCord
Sandia National Laboratory
Division 6416
P.O. Box 5800
Albuquerque, NM 87185

D. B. McLaughlin
Ralph M. Parsons Laboratory, 48-209
Department of Civil Engineering
Massachusetts Institute of Technology
Cambridge, MA 02139

Ed Mehnert
Illinois State Geological Survey
Natural Resources Building
615 E. Peabody Dr.
Champaign, IL 61820

O. Mendiratta
West Valley Nuclear Services
P.O. Box 191, MS-AA9
West Valley, NY 14171-0191

J. W. Mercer
GeoTrans, Inc.
46050 Manekin Plaza
Suite 100
Sterling, VA 22170

W. Meyers
District Chief
U.S. Geological Survey, WRD
677 Ala Moana Blvd., Suite 415
Honolulu, HI 96813

H. J. Morel-Seytoux
57 Selby Lane
Atherton, CA 94027-3926

L. Morton
Utah Division of Radiation Control
P.O. Box 144850
Salt Lake City, UT 84114-4850

S. P. Neuman
Department of Hydrology and Water Resources
University of Arizona
Tucson, AZ 85721

J. E. Odencrantz
Tri-S Envirnomental Corp.
2121 Yacht Yankee
Newport Beach, CA 92660-6728

J. S. Oldow
Geology Department
University of Idaho
Moscow, ID 83843

A. Padgett
N.C. DRP
1325 Stapleton Dr.
Garner, NC 27529

A. O. Perry
Bureau of Mines
MS 6205
810 Seventh St., NW
Washington, DC 20241

G. F. Pinder
College of Engineering and Mathematics
University of Vermont
Burlington, VT 05405

K. Pruess
Lawrence Berkeley Laboratory
1 Cyclotron Road
Berkeley, CA 94720

D. R. Ralston
Geology Department
University of Idaho
Moscow, ID 83843

V. Rogers
Rogers & Associates Engineering Corp.
P.O. Box 330
Salt Lake City, UT 84107

B. Ross
Disposal Safety Incorporated
1660 L Street NW, Suite 314
Washington, DC 20036

F. Ross
U.S. Nuclear Regulatory Commission
11555 Rockville Pike
Rockville, MD 20852

M. H. Roulier
U.S. EPA Center Hill Facility
5995 Center Hill Ave.
Cincinnati, OH 45224

C. Rupert
Clean Water Fund of North Carolina
P.O. Box 1008
Raleigh, NC 27602

B. Sagar
Center for Nuclear Waste Regulatory Analysis
6220 Culebra Road
P.O. Drawer 28500
San Antonio, TX 78284

B. Scanlon
Bureau of Economic Geology
University of Texas
University Station Box X
Austin, TX 78713-7508

J. B. Sisson
Lockheed-Martin
P.O. Box 1625, MS 2107
Idaho Falls, ID 83415

E. T. Smith
U.S. Geological Survey
407 National Center
Reston, VA 22092
M. L. Smith
Metallurgical & Mining Engineering Dept.
University of Idaho
Moscow, ID 83843

F. Snider
405 North Mendenhall St.
Greensboro, NC 27401

E. P. Springer
Environmental Science Group
HSE 12
Health, Safety and Environment Division
Los Alamos National Laboratory
Los Alamos, NM 87545

D. B. Stephens
Daniel B. Stephens and Associates, Inc.
6020 Academy NE, Suite 100
Albuquerque, NM 87109

M. Stephens
AECL Research
Chalk River Laboratories, Station 15
Chalk River, Ontario
Canada K0J1J0

M. Thaggard
U.S. Nuclear Regulatory Commission
11555 Rockville Pike
Rockville, MD 20852

A. F. B. Tompson
Earth Sciences Department
L-206
Lawrence Livermore National Laboratory
Livermore, CA 94551

L. R. Townley
CSIRO, Division of Water Resources
Private Bag
PO Wembly WA 6014
Australia

N. Trask
US Geological Survey
Water Resources Division
411 National Center
Reston, VA 22092

C.-F. Tsang
Lawrence Berkeley Laboratory
1 Cyclotron Road
Berkeley, CA 94720

S. W. Tyler
Desert Research Institute
P.O. Box 60220
Reno, NV 89506

J. G. Uber
University of Cincinnati
Dept. of Civil & Environmental Engineering
ML 71
Cincinnati, OH 45221-0071

M. Th. van Genuchten
U.S. Salinity Lab - USDA
4500 Glenwood Drive
Riverside, CA 92501

B. K. Vodolaga
Institute of Technical Physics, VNIITF
456770
Snezhinsk (Chelyabinsk-70)
P.O. Box 245
Russia

C. F. Voss
Golder Associates, Inc.
4104 148th Ave. NE
Redmond, WA 98052

J.S.Y. Wang
Lawrence Berkeley Laboratory
1 Cyclotron Road
Berkeley, CA 94720

Art Warrick
Dept. of Soil and Water Science
429 Shantz Bldg.
University of Arizona
Tucson, AZ 85721

W. J. Waugh
Rust GeoTech
P.O. Box 14000
Grand Junction, CO 81502

E. P. Weeks
U.S. Geological Survey
Federal Center Mail Stop 413
Denver, CO 80225

P. J. Wierenga
Dept. of Soil and Water Science
429 Shantz Bldg.
University of Arizona
Tucson, AZ 85721

E. Wilhite
Westinghouse Savannah River Co.
773-A P.O. Box 616
Aiken, SC 29802

R. E. Williams (5)
Geology Department
University of Idaho
Moscow, ID 83843

P. A. Witherspoon
Lawrence Berkeley Laboratory
1 Cyclotron Road
Berkeley, CA 94720

Man-Sung Yim
Massachusetts Institute of Technology
77 Massachusetts Ave.
Rm. 24-214
Cambridge, MA 02139

M. H. Young
Dept. of Soil and Water Science
429 Shantz Bldg.
University of Arizona
Tucson, AZ 85721

ONSITE

Westinghouse Hanford Company
N. W. Kline H0-36
F. M. Mann H0-36

Bechtel Hanford
M. P. Connelly X0-37

WSU Tri-Cities
J. L. Conca H2-52

Pacific Northwest Laboratory (38)
N. J. Aimo
M. P. Bergeron
D. J. Bradley
J. W. Cary
A. Chilakapati
C. R. Cole
R. M. Ecker
M. J. Fayer
M. G. Foley
M. D. Freshley
G. W. Gee
T. R. Ginn
J. O. Heaberlin
C. T. Kincaid
R. R. Kirkham
R. E. Lewis
P. D. Meyer
W. E. Nichols
M. L. Rockhold
B. D. Shipp
C. S. Simmons
R. L. Skaggs
J. L. Smoot (5)
G. P. Streile
J. E. Szecsody
A. L. Ward
M. D. White
Information Release (7)

NRC FORM 335 (2-89) NRCM 1102, 3201, 3202

U.S. NUCLEAR REGULATORY COMMISSION

BIBLIOGRAPHIC DATA SHEET

(See instructions on the reverse)

1. REPORT NUMBER (Assigned by NRC. Add Vol., Supp., Rev., and Addendum Numbers, if any.)
NUREG/CR-6411
PNL - 10866

2. TITLE AND SUBTITLE
A Geostatistical Methodology to Assess the Accuracy of Unsaturated Flow Models

3. DATE REPORT PUBLISHED
MONTH: April
YEAR: 1996

4. FIN OR GRANT NUMBER
L2466

5. AUTHOR(S)
JL Smoot
RE Williams

6. TYPE OF REPORT
Technical

7. PERIOD COVERED *(Inclusive Dates)*

8. PERFORMING ORGANIZATION – NAME AND ADDRESS *(If NRC, provide Division, Office or Region, U.S. Nuclear Regulatory Commission, and mailing address; if contractor, provide name and mailing address.)*
Pacific Northwest National Laboratory
P.O. Box 999
Richland, WA 99352

9. SPONSORING ORGANIZATION – NAME AND ADDRESS *(If NRC, type "Same as above"; if contractor, provide NRC Division, Office or Region, U.S. Nuclear Regulatory Commission, and mailing address.)*
Division of Regulatory Applications
Office of Nuclear Regulatory Research
U.S. Nuclear Regulatory Commission
Washington, DC 20551-0001

10. SUPPLEMENTARY NOTES
T. Nicholson, NRC Project Manager

11. ABSTRACT *(200 words or less)*

The Pacific Northwest National Laboratory (PNNL) has developed a Hydrologic Evaluation Methodology (HEM) to assist the U.S. Nuclear Regulatory Commission in evaluating the potential that infiltrating meteoric water will produce leachate at commercial low-level radioactive waste disposal sites. Two key issues are raised in the HEM: 1) evaluation of mathematical models that predict facility performance, and 2) estimation of the uncertainty associated with these mathematical model predictions. The technical objective of this research is to adapt geostatistical tools commonly used for model parameter estimation to the problem of estimating the spatial distribution of the dependent variable to be calculated by the model. To fulfill this objective, a database describing the spatiotemporal movement of water injected into unsaturated sediments at the Hanford Site in Washington State was used to develop a new method for evaluating mathematical model predictions. Measured water content data were interpolated geostatisically to a 16 x 16 x 36 grid at several time intervals. Then a mathematical model was used to predict water content at the same grid locations at the selected times. Node-by-node comparison of the mathematical model predictions with the geostatistically interpolated values was conducted. The method facilitates a complete accounting and categorization of model error at every node. The comparison suggests that model results generally are within measurement error. The worst model error occurs in silt lenses and is in excess of measurement error.

12. KEY WORDS/DESCRIPTORS *(List words or phrases that will assist researchers in locating the report.)*
Hydrology
Unsaturated Zone
Geostatistics
Three-Dimensional Numerical Model
Three-Dimensional Visualization

13. AVAILABILITY STATEMENT
Unlimited

14. SECURITY CLASSIFICATION
(This Page)
Unclassified
(This Report)
Unclassified

15. NUMBER OF PAGES

16. PRICE

Federal Recycling Program